

## TOTAL POSITIVITY IN MULTIVARIATE EXTREMES

FRANK RÖTTGER, SEBASTIAN ENGELKE, AND PIOTR ZWIERNIK

**ABSTRACT.** Positive dependence is present in many real world data sets and has appealing stochastic properties. In particular, the notion of multivariate total positivity of order 2 (MTP<sub>2</sub>) is a convex constraint and acts as an implicit regularizer in the Gaussian case. We study positive dependence in multivariate extremes and introduce EMTP<sub>2</sub>, an extremal version of MTP<sub>2</sub>. This notion turns out to appear prominently in extremes and, in fact, it is satisfied by many classical models. For a Hüsler–Reiss distribution, the analogue of a Gaussian distribution in extremes, we show that it is EMTP<sub>2</sub> if and only if its precision matrix is a Laplacian of a connected graph. We propose an estimator for the parameters of the Hüsler–Reiss distribution under EMTP<sub>2</sub> as the solution of a convex optimization problem with Laplacian constraint. We prove that this estimator is consistent and typically yields a sparse model with possibly non-decomposable extremal graphical structure. At the example of two data sets, we illustrate this regularization and the superior performance compared to existing methods.

## 1. INTRODUCTION

Positive dependence has been extensively studied in the multivariate dependence modeling literature. It has important applications in probability theory and statistical physics; see, for example, (Fortuin et al., 1971; Newman, 1983, 1984). A particularly important notion is multivariate total positivity of order 2 (MTP<sub>2</sub>) (Karlin and Rinott, 1980; Fallat et al., 2017). Recently there is surging interest in this and related concepts in connection with sparsity and high-dimensional modeling (Slawski and Hein, 2015; Lauritzen et al., 2019; Lauritzen and Zwiernik, 2020b). Even though in a probabilistic sense the MTP<sub>2</sub> property implies rather restrictive conditions on the models, in many data sets MTP<sub>2</sub> seems to be naturally present. Agrawal et al. (2020) show that for portfolio selection, maximum likelihood estimation under MTP<sub>2</sub> outperforms many state-of-the-art methods, and Wang et al. (2020) and Rossell and Zwiernik (2021) investigate total positivity in a S&P500 dataset. Other recent examples are from psychometrics (Lauritzen et al., 2019, 2021), evolution and phylogenetics (Slawski and Hein, 2015; Sturmfels et al., 2020), and machine learning (Ying et al., 2021; Egilmez et al., 2017). The machine learning applications exploit the connection to graph Laplacians, which will be also important here. For more detailed theoretical analysis of the MTP<sub>2</sub> constraint we refer to Fallat et al. (2017).

When interest is in the dependence of extreme events, such as during a crisis on the stock market, then intuitively one may expect even stronger positive dependence than in normal times. In this paper we follow this intuition and formalize positive dependence for extremes. For multivariate Pareto distributions, which are the only possible limits for multivariate threshold exceedances (Rootzén and Tajvidi, 2006), we propose a natural notion of MTP<sub>2</sub> that we call extremal MTP<sub>2</sub> (EMTP<sub>2</sub>). In order to characterize EMTP<sub>2</sub> we establish new additive relations of positive dependence, which are of independent interest. For a random variable  $X_0$  that is independent of a random vector  $\mathbf{X}$ , we define

$$\mathbf{Y} = (X_0, \mathbf{X} + X_0 \mathbf{1}),$$

with  $\mathbf{1}$  being the vector of ones, and link the probabilistic dependence properties of the vectors  $\mathbf{X}$  and  $\mathbf{Y}$ . For instance,  $\mathbf{Y}$  is MTP<sub>2</sub> if and only if  $\mathbf{X}$  is strongly MTP<sub>2</sub>; the latter is also known as LLC in the literature (Murota, 2009; Robeva et al., 2021).

As intuition suggests, positive dependence in general and our EMTP<sub>2</sub> in particular naturally arise in the study of multivariate extremes. Indeed, many of the classical models such as the extremal logistic (Tawn, 1990) and Dirichlet distributions (Coles and Tawn, 1991) are EMTP<sub>2</sub> across the whole range of their parameter values and in any dimension.

Within the multivariate Pareto distributions, the class of Hüsler–Reiss models parameterized by a variogram matrix  $\Gamma$  can be seen as the counterpart of Gaussian models in multivariate extremes. An alternative parameterization is given in terms of the Hüsler–Reiss precision matrices  $\Theta$  defined by Hentschel (2021). Inside this class, we show that a model is EMTP<sub>2</sub> if its precision matrix  $\Theta$  is a Laplacian matrix of a connected graph with positive edge weights, that is,  $\Theta_{ij} \leq 0$  for all  $i \neq j$ . In particular, this implies that any bivariate and any tree structured Hüsler–Reiss distribution is EMTP<sub>2</sub>. We also study a weaker form of positive dependence, extremal association, and show that it is satisfied for a Hüsler–Reiss model if and only if  $\Gamma$  satisfies the triangle inequality  $\Gamma_{ij} \leq \Gamma_{ik} + \Gamma_{jk}$  for all  $i, j, k$ , and thus is a metric. This result may be of independent interest in relation to the work on effective resistance in electrical networks and so called resistance distances on graphs (Fiedler, 1998; Devriendt, 2020; Klein and Randić, 1993). To supplement this work, our paper gives the exact condition and a probabilistic interpretation for the case when  $\Gamma$  is a metric.

The statistical analysis of extreme events is challenging since, by definition, only the largest observations carry relevant information. For this reason, recent advances in multivariate extremes concentrate on defining and detecting sparse structures in the distributional tails (e.g., Gissibl and Klüppelberg, 2018; Janßen and Wan, 2020; Segers, 2020; Drees and Sabourin, 2021); for a review see Engelke and Ivanovs (2021). One approach to sparse extreme value modeling is to study conditional independence and graphical models for multivariate Pareto distributions (Engelke and Hitz, 2020). Our EMTP<sub>2</sub> notion is well compatible with these extremal graphical models and in particular the case of trees seems natural and has interesting connections to Brownian motion tree models (Felsenstein, 1973; Sturmfels et al., 2020). We further study the axiomatization of extremal conditional independence in the spirit of Fallat et al. (2017) and Lauritzen and Sadeghi (2018), and show that EMTP<sub>2</sub> graphical models satisfy an extremal notion of faithfulness.

We propose an estimator of the Hüsler–Reiss precision matrix  $\Theta$  that takes the empirical version of the variogram  $\bar{\Gamma}$  as input and minimizes the convex problem

$$-\log \text{Det } \Theta + \frac{1}{2} \text{tr}(\bar{\Gamma}\Theta),$$

over all positive semi-definite precision matrices and under the EMTP<sub>2</sub> constraint that  $\Theta$  is a Laplacian matrix of a connected graph with positive edge weights. Here,  $\text{Det}$  denotes the pseudo-determinant since  $\Theta$  has one zero eigenvalue. We prove the consistency of this estimator, and based on the dual formulation we design a block coordinate-descent algorithm that efficiently solves the constrained optimization problem. The EMTP<sub>2</sub> constraint acts as an implicit regularizer and the estimator can also be applied in high-dimensional settings. Moreover, since the solution satisfies certain KKT conditions for optimality, the estimator  $\hat{\Theta}$  under EMTP<sub>2</sub> typically contains zeros, which implies that the corresponding Hüsler–Reiss model is an extremal graphical model. In particular, the resulting graph can have any, possibly non-decomposable structure and is therefore much more general than the block graphs considered in Engelke and Hitz (2020). This relates to several discussion contributions of the latter paper that point out practical limitations of block graphs.

As an illustration of our method we consider the `carcass` data set (Højsgaard et al., 2012), which exhibits positive dependence in the Gaussian case (Lauritzen et al., 2019). To further assess the

statistical performance of our EMTP<sub>2</sub> estimator, we apply it to a data set of river discharges and compare it to methods from spatial statistics (Asadi et al., 2015) and graphical modeling (Engelke and Hitz, 2020).

## 2. NOTIONS OF POSITIVE DEPENDENCE

In this section we recall some notions of positive dependence, with a focus on multivariate total positivity of order 2; see Karlin and Rinott (1980) for more details. Our version of total positivity for extremes builds upon this notion. A detailed treatment of extremal MTP<sub>2</sub> requires the study of a stronger notion of positive dependence, which we call strong MTP<sub>2</sub>.

**2.1. Definitions and basic properties.** Let  $\mathbf{x} \vee \mathbf{y}$  denote the componentwise maximum and  $\mathbf{x} \wedge \mathbf{y}$  the componentwise minimum for vectors  $\mathbf{x}, \mathbf{y} \in \mathbb{R}^d$ . A function  $f : \mathbb{R}^d \rightarrow \mathbb{R}$  is *multivariate totally positive of order 2* (MTP<sub>2</sub>) if

$$(1) \quad f(\mathbf{x} \vee \mathbf{y})f(\mathbf{x} \wedge \mathbf{y}) \geq f(\mathbf{x})f(\mathbf{y}) \quad \text{for all } \mathbf{x}, \mathbf{y} \in \mathbb{R}^d.$$

We say that  $f$  is strongly MTP<sub>2</sub> if

$$(2) \quad f(\mathbf{x} \vee (\mathbf{y} - \alpha \mathbf{1}))f((\mathbf{x} + \alpha \mathbf{1}) \wedge \mathbf{y}) \geq f(\mathbf{x})f(\mathbf{y}) \quad \text{for all } \mathbf{x}, \mathbf{y} \in \mathbb{R}^d, \alpha \geq 0,$$

where  $\mathbf{1}$  denotes the vector of ones. A multivariate random vector  $\mathbf{X}$  with density  $f_{\mathbf{X}}$  is MTP<sub>2</sub> if  $f_{\mathbf{X}}$  is MTP<sub>2</sub> and it is strongly MTP<sub>2</sub> if  $f_{\mathbf{X}}$  is strongly MTP<sub>2</sub>.

The concept of strongly MTP<sub>2</sub> distributions is relatively new and not well studied. In the statistical context (2) was used in Robeva et al. (2021), where strong MTP<sub>2</sub> is called log- $L^\#$ -concave (LLC) in reference to work on discrete optimization (e.g., Murota, 2009) where, in addition,  $f$  is assumed to be log-concave. Here, a non-negative function is log-concave if its logarithm is a concave function. A random vector  $\mathbf{X}$  is log-concave if its density is log-concave. For a list of further references for the appearance of strong MTP<sub>2</sub> in applications, see Robeva et al. (2021, p.3-4).

A further notion of positive dependence is association. We recall that a random vector  $\mathbf{X} = (X_1, \dots, X_n)$  is associated if  $\text{Cov}(f(\mathbf{X}), g(\mathbf{X})) \geq 0$  for any two non-decreasing functions  $f, g : \mathbb{R}^d \rightarrow \mathbb{R}$  for which this covariance exists; see Esary et al. (1967) for more details. Note that MTP<sub>2</sub> implies association (Fortuin et al., 1971).

**Example 1.** If  $\mathbf{X}$  is Gaussian with mean vector  $\mu$  and invertible covariance matrix  $\Sigma$ , then  $\mathbf{X}$  is MTP<sub>2</sub> if and only if the inverse covariance matrix  $K$  is an *M-matrix*, that is, a positive definite matrix such that  $K_{ij} \leq 0$ ; see for example Lauritzen et al. (2019). Moreover,  $\mathbf{X}$  is strongly MTP<sub>2</sub> if, in addition,  $K$  is a diagonally dominant matrix, that is, all row sums are nonnegative ( $K\mathbf{1} \geq \mathbf{0}$ ); see Robeva et al. (2021). Finally,  $\mathbf{X}$  is associated if and only if  $\Sigma$  has only non-negative entries (Pitt, 1982).

**Remark 2.1.** This example generalizes. An alternative characterization of MTP<sub>2</sub> and strong MTP<sub>2</sub> for random vectors with a positive twice-differentiable log-concave density  $f(\mathbf{x})$  is that  $\mathbf{X}$  is (strongly) MTP<sub>2</sub> if and only if the Hessian matrix of  $-\log f(\mathbf{x})$  is a (diagonally dominant) M-matrix, see Karlin and Rinott (1980) and Murota (2009, Equation (2.15)).

We are now ready to state and prove the main result of this section, which provides an important characterization of strongly MTP<sub>2</sub> distributions and other useful results. The proof relies on an equivalent formulation of the strongly MTP<sub>2</sub> condition, which we give in Lemma B.1. Recall that the support of a density function  $f$  is the smallest closed set over which the density integrates to 1.

**Theorem 2.2.** Let  $X_0$  be a random variable whose density is supported on  $[c, \infty)$  for some  $c \in \mathbb{R}$ , and let  $\mathbf{X} = (X_1, \dots, X_d)$  be a random vector such that  $X_0 \perp\!\!\!\perp \mathbf{X}$ . Let  $\mathbf{Y} = (X_0, \mathbf{X} + X_0 \mathbf{1})$ . Then:

$$(1) \quad \mathbf{Y} \text{ is MTP}_2 \iff \mathbf{X} \text{ is strongly MTP}_2.$$

- (2)  $\mathbf{Y}$  is strongly MTP<sub>2</sub>  $\iff X_0$  and  $\mathbf{X}$  are strongly MTP<sub>2</sub>.  
 (3)  $\mathbf{Y}$  is associated  $\iff \mathbf{X}$  is associated.

*Proof.* Observe that the density  $f$  of  $\mathbf{Y}$  satisfies

$$(3) \quad f(y_0, \mathbf{y}) = f_0(y_0) f_{\mathbf{X}}(\mathbf{y} - y_0 \mathbf{1}).$$

Proof of statement (1): Using (3), the MTP<sub>2</sub> constraint on  $f$  is equivalent to

$$(4) \quad f_{\mathbf{X}}(\mathbf{x} \vee \mathbf{y} - (x_0 \vee y_0) \mathbf{1}) f_X(\mathbf{x} \wedge \mathbf{y} - (x_0 \wedge y_0) \mathbf{1}) \geq f_{\mathbf{X}}(\mathbf{x} - x_0 \mathbf{1}) f_{\mathbf{X}}(\mathbf{y} - y_0 \mathbf{1})$$

for all  $(x_0, \mathbf{x}), (y_0, \mathbf{y})$ , where we used the fact that  $f_0(x_0) f_0(y_0) = f_0(x_0 \vee y_0) f_0(x_0 \wedge y_0)$  (with both sides non-zero). But this condition is exactly equivalent to  $f_{\mathbf{X}}$  being strongly MTP<sub>2</sub> by Lemma B.1.

Proof of statement (2): We first show the left implication via the equivalent characterization of strong MTP<sub>2</sub> from Lemma B.1. Denoting  $\bar{\mathbf{x}} = (x_0, \mathbf{x})$  and  $\bar{\mathbf{y}} = (y_0, \mathbf{y})$  we want to show that for every  $s \leq t$  it holds that

$$f(\bar{\mathbf{x}} - s \mathbf{1}) f(\bar{\mathbf{y}} - t \mathbf{1}) \leq f(\bar{\mathbf{x}} \wedge \bar{\mathbf{y}} - s \mathbf{1}) f(\bar{\mathbf{x}} \vee \bar{\mathbf{y}} - t \mathbf{1}).$$

The left hand side of this inequality is

$$L := f_0(x_0 - s) f_0(y_0 - t) f_X(\mathbf{x} - x_0 \mathbf{1}) f_X(\mathbf{y} - y_0 \mathbf{1})$$

and the right hand side is

$$R := f_0(x_0 \wedge y_0 - s) f_0(x_0 \vee y_0 - t) f_X(\mathbf{x} \wedge \mathbf{y} - (x_0 \wedge y_0) \mathbf{1}) f_X(\mathbf{x} \vee \mathbf{y} - (x_0 \vee y_0) \mathbf{1}).$$

In the proof of statement (1) we established that the strongly MTP<sub>2</sub> property of  $\mathbf{X}$  gives that  $\mathbf{Y}$  is MTP<sub>2</sub>. In other words, the inequality (4) holds. Given this inequality, to show  $L \leq R$  it is certainly enough to show that

$$f_0(x_0 - s) f_0(y_0 - t) \leq f_0(x_0 \wedge y_0 - s) f_0(x_0 \vee y_0 - t),$$

which holds if  $f_0$  is strongly MTP<sub>2</sub> by Lemma B.1. For the other direction, note that by statement (1), we have that  $\mathbf{X}$  is strongly MTP<sub>2</sub> as  $\mathbf{Y}$  is MTP<sub>2</sub>. To conclude that  $X_0$  is strongly MTP<sub>2</sub>, we will show that strongly MTP<sub>2</sub> distributions are closed under marginalization. This will conclude the proof of the second statement.

Strongly MTP<sub>2</sub> distributions are closed under taking margins: Suppose that  $\mathbf{Z} = (Z_1, \dots, Z_d)$  is strongly MTP<sub>2</sub>. We will show that  $(Z_1, \dots, Z_{d-1})$  is strongly MTP<sub>2</sub>. By statement (1),  $\mathbf{Z}$  is strongly MTP<sub>2</sub> if and only if for every  $X_0$  independent of  $\mathbf{Z}$  and supported on  $[c, \infty)$  for some fixed  $c \in \mathbb{R}$ , the vector  $(X_0, X_0 + Z_1, \dots, X_0 + Z_d)$  is MTP<sub>2</sub>. By the closure property of the MTP<sub>2</sub> distributions, the vector  $(X_0, X_0 + Z_1, \dots, X_0 + Z_{d-1})$  is also MTP<sub>2</sub> for every such  $X_0$ . Again using statement (1), this is equivalent to  $(Z_1, \dots, Z_{d-1})$  being strongly MTP<sub>2</sub>. The same argument applies to any other margin.

Proof of statement (3): For the left implication note that for any non-decreasing function  $f$  we have

$$f(\mathbf{Y}) = f(X_0, \mathbf{X} + X_0 \mathbf{1}) =: \tilde{f}(X_0, \mathbf{X}),$$

where  $\tilde{f}(x_0, \mathbf{x}) = f(x_0, \mathbf{x} + x_0 \mathbf{1})$  is then also non-decreasing. If  $\mathbf{X}$  is associated then  $(X_0, \mathbf{X})$  is associated by combining properties (ii) and (iii) in Proposition B.2. Thus, for any two non-decreasing functions  $f, g : \mathbb{R}^{d+1} \rightarrow \mathbb{R}$  we have

$$\text{Cov}(f(\mathbf{Y}), g(\mathbf{Y})) = \text{Cov}(\tilde{f}(X_0, \mathbf{X}), \tilde{g}(X_0, \mathbf{X})) \geq 0.$$

The last inequality follows by association of  $(X_0, \mathbf{X})$  and the fact that  $\tilde{f}, \tilde{g}$  are non-decreasing. Association of  $\mathbf{Y}$  follows.

For the right implication let  $\mathbf{Z} = (Y_1, \dots, Y_d)$  with  $\mathbf{Z} = \mathbf{X} + X_0 \mathbf{1}$ . By assumption,  $\mathbf{Y} = (Y_0, \mathbf{Z})$  is associated. By the law of total covariance, for any two non-decreasing  $f, g : \mathbb{R}^d \rightarrow \mathbb{R}$ , we have

$$\begin{aligned} \text{Cov}(f(\mathbf{X}), g(\mathbf{X})) &= \text{Cov}(f(\mathbf{Z} - Y_0 \mathbf{1}), g(\mathbf{Z} - Y_0 \mathbf{1})) \\ &= \mathbb{E} \left[ \text{Cov}(f(\mathbf{Z} - Y_0 \mathbf{1}), g(\mathbf{Z} - Y_0 \mathbf{1}) | Y_0) \right] + \text{Cov}(\mathbb{E}[f(\mathbf{Z} - Y_0 \mathbf{1}) | Y_0], \mathbb{E}[g(\mathbf{Z} - Y_0 \mathbf{1}) | Y_0]). \end{aligned}$$

If  $\mathbf{Y}$  is associated then  $\mathbf{Z}$  is associated by Proposition B.2(i). It follows that the conditional covariance in the first summand is non-negative. To show that the second term is also non-negative we observe that the functions  $-\mathbb{E}[f(\mathbf{Z} - Y_0 \mathbf{1}) | Y_0]$  and  $-\mathbb{E}[g(\mathbf{Z} - Y_0 \mathbf{1}) | Y_0]$  are both non-decreasing in  $Y_0$ . Since  $Y_0$  is associated by Proposition B.2(iii),

$$\text{Cov}(\mathbb{E}[f(\mathbf{Z} - Y_0 \mathbf{1}) | Y_0], \mathbb{E}[g(\mathbf{Z} - Y_0 \mathbf{1}) | Y_0]) = \text{Cov}(-\mathbb{E}[f(\mathbf{Z} - Y_0 \mathbf{1}) | Y_0], -\mathbb{E}[g(\mathbf{Z} - Y_0 \mathbf{1}) | Y_0]) \geq 0.$$

This shows association of  $\mathbf{X}$  and completes the proof.  $\square$

Proving Theorem 2.2 we showed that strong  $\text{MTP}_2$  is closed under taking margins. The corresponding statements for association and  $\text{MTP}_2$  are well known.

**Proposition 2.3.** *The following three statements hold.*

- (1) *If  $\mathbf{X}$  is  $\text{MTP}_2$  then every margin of  $\mathbf{X}$  is  $\text{MTP}_2$ .*
- (2) *If  $\mathbf{X}$  is strongly  $\text{MTP}_2$  then every margin of  $\mathbf{X}$  is strongly  $\text{MTP}_2$ .*
- (3) *If  $\mathbf{X}$  is associated then every margin of  $\mathbf{X}$  is associated.*

*Proof.* The first statement is well known (e.g., Karlin and Rinott, 1980). The second statement is new and was shown in the proof of Theorem 2.2. The last statement was shown by Esary et al. (1967).  $\square$

So far log-concavity did not play any role in our analysis of strongly  $\text{MTP}_2$  distributions. The following lemma explains how log-concavity enters the picture.

**Lemma 2.4.** *A univariate distribution with density  $f : \mathbb{R} \rightarrow \mathbb{R}$  is strongly  $\text{MTP}_2$  if and only if it is log-concave. A random vector  $\mathbf{X} = (X_1, \dots, X_d)$  with independent components is strongly  $\text{MTP}_2$  if and only if each  $X_i$  is log-concave.*

*Proof.* Note that (2) with  $d = 1$  becomes non-trivial only if  $0 \leq \alpha \leq y - x$  in which case it gives  $f(y - \alpha)f(x + \alpha) - f(x)f(y) \geq 0$ . Let  $F : \mathbb{R} \rightarrow \mathbb{R} \cup \{-\infty\}$  be defined by  $F(x) = -\log f(x)$ . Denoting  $\alpha = \lambda(y - x)$  for  $\lambda \in [0, 1]$  we get

$$(F((1 - \lambda)x + \lambda y) - (1 - \lambda)F(x) - \lambda F(y)) + (F(\lambda x + (1 - \lambda)y) - \lambda F(x) - (1 - \lambda)F(y)) \leq 0.$$

Taking  $\lambda = \frac{1}{2}$  we conclude midpoint convexity of  $F$ , which is equivalent to concavity as  $x < y$  are arbitrary. On the other hand, convexity of  $F$  trivially implies the above inequality which is equivalent to the strongly  $\text{MTP}_2$  inequality.

For the second statement, let  $F(\mathbf{x}) = -\log f_X(\mathbf{x})$ , so that  $F(\mathbf{x}) = \sum_i F_i(x_i)$ , where  $F_i = -\log f_i$ . We want to show that for each  $\mathbf{x}, \mathbf{y} \in \mathbb{R}^d$ ,  $\alpha \geq 0$

$$\sum_i (F_i(x_i) + F_i(y_i) - F_i(x_i \vee (y_i - \alpha)) - F_i((x_i + \alpha) \wedge y_i)) \geq 0$$

if and only if each summand is non-negative. The left implication is obvious. But the right implication is also clear using the insights of the proof of the univariate case. Simply take  $\mathbf{x}, \mathbf{y}$  such that  $x_i > y_i$  for all  $i \neq k$ . The corresponding summands are zero and so necessarily  $F_k(x_k) + F_k(y_k) - F_k(x_k \vee (y_k - \alpha)) - F_k((x_k + \alpha) \wedge y_k) \geq 0$ .  $\square$

**2.2. Log-concave tree processes.** Theorem 2.2 gives a natural way to construct multivariate strongly MTP<sub>2</sub> distributions with log-concave distributions. If  $X_1, \dots, X_d$  are univariate log-concave then

$$(5) \quad (X_1, X_1 + X_2, X_1 + X_2 + X_3, \dots, X_1 + \dots + X_d)$$

is strongly MTP<sub>2</sub> and log-concave. We now provide a generalization of this construction.

Let  $T = (V, E)$  be an undirected tree with vertex set  $V = \{1, \dots, d\}$ . A rooted tree  $T^k$  is a tree obtained from  $T$  by choosing a vertex  $k \in V$ , called the root, and directing all edges away from  $k$ . For any two nodes  $i, j$  in an undirected tree  $T$  we denote by  $\text{ph}(ij; T)$  the set of edges on the (unique) path between  $i$  and  $j$  in this tree. Equivalently, for a rooted tree  $T^k$ , let  $\text{ph}(ij; T^k)$  be the set of directed edges on the (unique) path from  $i$  to  $j$  in  $T^k$ .

**Definition 1.** For a given rooted tree  $T^k$  with vertices  $V = \{1, \dots, d\}$  let  $X_1, \dots, X_d$  be a collection of independent random variables. Let  $\mathbf{Z} = (Z_1, \dots, Z_d)$  be defined by

$$(6) \quad Z_i = X_k + \sum_{uv \in \text{ph}(ki; T^k)} X_v,$$

where  $uv$  denotes a directed edge  $u \rightarrow v$ . Then we say that  $\mathbf{Z}$  follows an additive process on  $T^k$ . If all  $X_i$  are log-concave then we call such process a log-concave process on a tree.

For example, if  $d = 3$ , the vector in (5) forms an additive process on the tree  $1 \rightarrow 2 \rightarrow 3$ . Rerooting this tree at 2 results in an additive process  $(X_1 + X_2, X_2, X_2 + X_3)$ .

**Proposition 2.5.** *If  $\mathbf{Z}$  follows a log-concave tree process then it has a strongly MTP<sub>2</sub> and log-concave distribution.*

*Proof.* Since  $X_k$  is log-concave then by Theorem 2.2 the vector  $\mathbf{Z}$  is strongly MTP<sub>2</sub> as long as  $(Z_i - Z_k)_{i \neq k}$  is strongly MTP<sub>2</sub>. This vector can be split into independent components indexed by the children of  $k$  in  $T^k$ . In each of the components we apply the same argument recursively. The fact that concatenating independent strongly MTP<sub>2</sub> vectors gives a strongly MTP<sub>2</sub> vector is clear.  $\square$

A special case of the construction in Proposition 2.5 is when  $\mathbf{X}$  is independent zero-mean Gaussian. In this case, the set of marginal distributions over the leaves of  $T$  is called the Brownian motion tree model (Felsenstein, 1973); see, for example, Section 2 in Sturmfels et al. (2020) for the structural equation representation as in (6). Since the distribution of  $\mathbf{Y}$  is strongly MTP<sub>2</sub>, this property is preserved in the margin by Proposition 2.3. We recover a well-known fact that the inverse covariance matrix in a Brownian motion tree model is always a diagonally dominant M-matrix; see for example Dellacherie et al. (2014), where the covariance matrices in the Brownian motion tree model are called simply tree matrices. In extreme value theory, we encounter such construction in the context of the extremal tree models (see Section 5.5).

### 3. MULTIVARIATE PARETO DISTRIBUTIONS

This section briefly introduces the theory of multivariate Pareto distributions. For more details and references, see Engelke and Hitz (2020).

**3.1. Definition and properties.** Multivariate extreme value theory studies the tail properties of the distribution of a random vector  $\mathbf{X} = (X_1, \dots, X_d)$ . Since the univariate theory is well-studied (e.g., Embrechts et al., 1997; de Haan and Ferreira, 2006), it is common to normalize the margins to concentrate on the extremal dependence between the different components. In the sequel and throughout this paper, we assume that each component of  $\mathbf{X}$  has been normalized to have standard

Pareto distributions with distribution function  $1 - 1/x$ ,  $x > 1$ ; we discuss this normalization in more detail in the preprocessing steps of the application in Section 8.1.

In order to describe the extremal dependence structure, the assumption of multivariate regular variation is widely used (Resnick, 2008). Formally, it is satisfied if the limit

$$(7) \quad \lim_{u \rightarrow \infty} u[1 - \mathbb{P}(\mathbf{X} \leq u\mathbf{z})] = \Lambda(\mathbf{z})$$

exists for all  $\mathbf{z} \in \mathcal{E} = [0, \infty)^d \setminus \{\mathbf{0}\}$ . The exponent measure  $\Lambda$  is a Radon measure on  $\mathcal{E}$ . The fact that  $\Lambda$  arises as a limit in (7) implies that it is homogeneous of order  $-1$ , that is,  $\Lambda(t\mathbf{z}) = t^{-1}\Lambda(\mathbf{z})$ , for any  $t > 0$ . Throughout the paper, we assume that  $\Lambda$  possesses a positive Lebesgue density  $\lambda$ , which then is homogeneous of order  $-(d+1)$ , that is,  $\lambda(t\mathbf{y}) = t^{-(d+1)}\lambda(\mathbf{y})$  for any  $t > 0$  and  $\mathbf{y} \in \mathcal{E}$ . The  $I$ th marginal  $\lambda_I$  of  $\lambda$  is defined for any nonempty  $I \subset [d] := \{1, \dots, d\}$ , as usual by integrating out all components in  $[d] \setminus I$ , and it can be seen to be homogeneous of order  $-(|I|+1)$ .

We assume that  $\mathbf{X}$  is multivariate regularly varying. Multivariate regular variation is important since it implies that the distribution of the exceedances of  $\mathbf{X}$  over a high threshold converges to a so-called multivariate Pareto distribution  $\mathbf{Y}$  (Rootzén and Tajvidi, 2006), that is,

$$(8) \quad \mathbb{P}(\mathbf{Y} \leq \mathbf{z}) = \lim_{u \rightarrow \infty} \mathbb{P}(\mathbf{X}/u \leq \mathbf{z} \mid \|\mathbf{X}\|_\infty > u) = \frac{\Lambda(\mathbf{z} \wedge \mathbf{1}) - \Lambda(\mathbf{z})}{\Lambda(\mathbf{1})}, \quad \mathbf{z} \in \mathcal{L}.$$

The distribution of  $\mathbf{Y}$  is supported on the space

$$(9) \quad \mathcal{L} = \{\mathbf{x} \geq \mathbf{0} : \|\mathbf{x}\|_\infty > 1\},$$

and it can be expressed via the exponent measure  $\Lambda$ . Since we assume  $\Lambda$  to possess a density, also  $\mathbf{Y}$  admits a Lebesgue density that is given by  $f_Y(\mathbf{y}) = \lambda(\mathbf{y})/\Lambda(\mathbf{1})$ . If the convergence in (8) holds, we say that the random vector  $\mathbf{X}$  is in the domain of attraction of the multivariate Pareto distribution  $\mathbf{Y}$ .

The multivariate Pareto distribution  $\mathbf{Y}$  is defined on the non-product space  $\mathcal{L}$  defined in (9). In order to define stochastic properties for  $\mathbf{Y}$ , it will be convenient to work with the conditional random vectors

$$\mathbf{Y}^k = \mathbf{Y} \mid \{Y_k > 1\},$$

where  $k \in [d]$ . The random vector  $\mathbf{Y}^k$  has Lebesgue density  $\lambda$  supported on the product space  $\mathcal{L}^k = \{\mathbf{x} \in \mathcal{L} : x_k > 1\}$ . Thanks to the homogeneity of  $\Lambda$ , we have the stochastic representation

$$(10) \quad \mathbf{Y}^k \stackrel{d}{=} P\mathbf{W}^k,$$

where  $P$  has a standard Pareto distribution that is independent of a  $d$ -variate random vector  $\mathbf{W}^k$ . The latter is called the  $k$ th extremal function and it satisfies  $W_k^k = 1$  almost surely. We refer to Dombry and Eyi-Minko (2013), Dombry et al. (2016) and Engelke and Hitz (2020) for more background on extremal functions.

**Remark 3.1.** Alternatively, a multivariate Pareto distribution can be defined as a random vector  $\mathbf{Y}$  on  $\mathcal{L}$  whose distribution function is homogeneous of order  $-1$  and that satisfies  $\mathbb{P}(Y_1 > 1) = \dots = \mathbb{P}(Y_d > 1)$ ; see Engelke and Volgushev (2020) for details.

**3.2. Hüsler–Reiss distributions.** An important example of a multivariate Pareto distribution is the Hüsler–Reiss distribution, which can be seen as the analogue of the Gaussian distribution inside the class of multivariate Pareto distributions. For a fixed  $d \in \mathbb{N}$ , let  $\mathbb{S}_0^d$  be the set of symmetric  $d \times d$ -matrices with zero diagonal. We say that  $\Gamma \in \mathbb{S}_0^d$  is a conditionally negative definite matrix if  $\mathbf{x}^T \Gamma \mathbf{x} \leq 0$  for all  $\mathbf{x} \in \mathbb{R}^d$  such that  $\mathbf{x}^T \mathbf{1} = 0$ . Moreover,  $\Gamma$  is strictly conditionally negative definite if the inequality is always strict unless  $\mathbf{x} = \mathbf{0}$ . We denote the cone of such matrices by  $\mathcal{C}^d \subset \mathbb{S}_0^d$ . In Appendix A we collect various results on such matrices, which will be useful in the next sections. Note that from here on, we will abbreviate singleton set  $\{k\}$  by  $k$  and index sets  $[d] \setminus k$  by  $\setminus k$ .



The  $d$ -variate Hüsler–Reiss distribution is a multivariate Pareto distribution parametrized by  $\Gamma \in \mathcal{C}^d$  (Hüsler and Reiss, 1989). In this case, the random vector  $\log \mathbf{W}_{\setminus k}^k$  in (10) has a  $(d-1)$ -dimensional normal distribution with mean vector  $-\text{diag}(\Sigma^{(k)})/2$  and covariance  $\Sigma^{(k)}$  obtained from  $\Gamma$  via the Farris transform (Farris et al., 1970)

$$(11) \quad \Sigma_{ij}^{(k)} = \frac{1}{2} (\Gamma_{ik} + \Gamma_{jk} - \Gamma_{ij}), \quad i, j \neq k;$$

see Engelke et al. (2015) for details. Note that (11) is a linear isomorphism from  $\mathbb{S}_0^d$  to the space  $\mathbb{S}^{d-1}$  of all symmetric  $(d-1) \times (d-1)$  matrices and its inverse is given by

$$(12) \quad \begin{cases} \Gamma_{ik} = \Sigma_{ii}^{(k)}, & i \neq k, \\ \Gamma_{ij} = \Sigma_{ii}^{(k)} + \Sigma_{jj}^{(k)} - 2\Sigma_{ij}^{(k)}, & i, j \neq k. \end{cases}$$

The fact that  $\Sigma^{(k)}$  is positive definite follows from the next result; for a proof see Lemma 3 in Engelke and Hitz (2020) or Lemma A.8 in Appendix A.

**Lemma 3.2.** *The image of the cone  $\mathcal{C}^d$  under the linear mapping (11) is the set of all positive definite matrices  $\mathbb{S}^{d-1}$ .*

In the multivariate Gaussian distribution the covariance matrix is the mean parameter and its inverse is the canonical parameter. Working with the inverse is useful as the log-likelihood function is a concave function. Analogously, a useful parameterization for the Hüsler–Reiss distribution is discussed in Hentschel (2021). Let  $\Theta^{(k)}$  denote the inverse of  $\Sigma^{(k)}$ . Define the matrix  $\Theta \in \mathbb{S}^d$  as

$$(13) \quad \Theta_{ij} := \Theta_{ij}^{(k)} \quad \text{for some } k \neq i, j.$$

Note that  $\Theta_{ij}^{(k)} = \Theta_{ij}^{(k')}$  for  $i, j \neq k, k'$  by Engelke and Hitz (2020, Lemma 1). An important alternative characterization of  $\Theta$  is obtained as follows. Define

$$(14) \quad \mathbf{P} := I_d - \frac{1}{d} \mathbf{1}\mathbf{1}^T$$

and let

$$(15) \quad \Sigma := \mathbf{P}(-\frac{\Gamma}{2})\mathbf{P}.$$

By Lemma A.6, if  $\Gamma \in \mathcal{C}^d$  then  $\Sigma$  is positive semi-definite. Moreover,  $\text{rank}(\Sigma) = d-1$  and  $\Sigma\mathbf{1} = \mathbf{0}$ . Denote by  $A^+$  the Moore–Penrose pseudoinverse of  $A$ .

**Proposition 3.3** (Hentschel (2021)). *Consider  $\Theta$  defined in (13) and  $\Sigma$  defined in (15). We have  $\Theta = \Sigma^+$ . It follows that  $\text{rank}(\Theta) = d-1$  and  $\Theta\mathbf{1} = \mathbf{0}$ .*

The matrix  $\Theta$  plays a particularly important role in connection with positive dependence. This will be discussed in the next section.

#### 4. EXTREMAL MTP<sub>2</sub> DISTRIBUTIONS

Total positivity in (1) is defined from an inequality where a probability density is evaluated at two points and their corresponding componentwise minimum and maximum. The space  $\mathcal{L}$  in the definition of multivariate Pareto distributions is not closed under these componentwise operations. It follows that the definition (1) is not directly applicable to multivariate Pareto distributions. Similar to extremal conditional independence (see Definition 3), we define extremal versions of MTP<sub>2</sub> and association.

**Definition 2.** Let  $\mathbf{Y}$  be a multivariate Pareto random vector. We say that  $\mathbf{Y}$  is extremal multivariate totally positive of order 2 (EMTP<sub>2</sub>) if and only if  $\mathbf{Y}^k$  is MTP<sub>2</sub> for all  $k \in [d]$ . Similarly, we say that  $\mathbf{Y}$  is extremal associated if and only if  $\mathbf{Y}^k$  is associated for all  $k \in [d]$ .



Clearly, as  $\text{MTP}_2$  implies association,  $\text{EMTP}_2$  implies extremal association.

As the exponent density  $\lambda$  is homogeneous of order  $-(d+1)$ , we obtain that the  $\text{MTP}_2$  property on a product space  $\mathcal{L}^k$  for one  $k \in [d]$  implies the same for any  $k \in [d]$  via a simple projection.

**Proposition 4.1.** *If  $\mathbf{Y}^k$  is  $\text{MTP}_2$  for some  $k \in [d]$ , it follows that  $\mathbf{Y}$  is  $\text{EMTP}_2$ .*

*Proof.*  $\mathbf{Y}^k$  has density  $\lambda(\mathbf{y})$  and is supported on the product space  $\mathcal{L}^k$ . Assume that  $\mathbf{Y}^k$  is  $\text{MTP}_2$ , that is, that  $\lambda(\mathbf{y})$  satisfies (1) on  $\mathcal{L}^k$ . For any  $k' \in [d]$  there exists some  $t > 0$  such that for any  $x, y \in \mathcal{L}^{k'}$  it holds that  $t\mathbf{x}, t\mathbf{y}, t(\mathbf{x} \wedge \mathbf{y}), t(\mathbf{x} \vee \mathbf{y}) \in \mathcal{L}^k$ . Hence, it follows from the homogeneity property of  $\lambda$  that

$$\begin{aligned} \lambda(\mathbf{x} \vee \mathbf{y})\lambda(\mathbf{x} \wedge \mathbf{y}) &= t^{2d+2}\lambda(t(\mathbf{x} \vee \mathbf{y}))\lambda(t(\mathbf{x} \wedge \mathbf{y})) \\ &\geq t^{2d+2}\lambda(t\mathbf{x})\lambda(t\mathbf{y}) \\ &= \lambda(\mathbf{x})\lambda(\mathbf{y}). \end{aligned}$$

□

Theorem 2.2 and the stochastic representation (10) give us a simple way of verifying whether  $\mathbf{Y}$  is  $\text{EMTP}_2$ . The following result shows how the strong  $\text{MTP}_2$  property becomes important in our setting.

**Theorem 4.2.** *A multivariate Pareto distribution  $\mathbf{Y}$  is  $\text{EMTP}_2$  if and only if the distribution of  $(\log \mathbf{W}_i^k)_{i \neq k}$  is strongly  $\text{MTP}_2$  for some  $k \in [d]$ .*

*Proof.* By Proposition 4.1 checking this condition on one  $k$  is sufficient so without loss of generality take  $k = d$ . By standard properties of  $\text{MTP}_2$  distributions,  $\mathbf{Y}^d$  is  $\text{MTP}_2$  if and only if its logarithm is  $\text{MTP}_2$  (follows directly from (1.13) in Karlin and Rinott (1980)). Using (10) we have  $\log Y_d^d = \log P$  and  $\log Y_i^d = \log P + \log W_i^d$  for  $i = 1, \dots, d-1$ . Since  $\log P$  is exponentially distributed, we can use Theorem 2.2 to conclude that  $\mathbf{Y}^d$  is  $\text{MTP}_2$  if and only if the vector  $(\log W_i^d)_{i \neq d}$  is strongly  $\text{MTP}_2$ . □

It follows that the  $\text{EMTP}_2$  property for multivariate Pareto distributions is completely characterized by their extremal functions. We will see in the following sections that this leads to simple constraints for  $\text{EMTP}_2$  to hold.

**4.1. Hüsler–Reiss distributions.** For the Hüsler–Reiss distribution, the extremal function is distributed according to a degenerate log-Gaussian distribution. Therefore, Theorem 4.2 gives us immediately the following result.

**Theorem 4.3.** *The Hüsler–Reiss distribution is  $\text{EMTP}_2$  if and only if the inverse of  $\Sigma^{(k)}$  in (11) is a diagonally dominant M-matrix for some  $k \in [d]$ .*

*Proof.* By Theorem 4.2 the random vector  $(\log W_i^k)_{i \neq k}$  must be strongly  $\text{MTP}_2$  for some  $k \in [d]$ . Since this vector is a  $(d-1)$ -variate Gaussian with covariance matrix  $\Sigma^{(k)}$ , equivalently the inverse  $\Theta^{(k)}$  of  $\Sigma^{(k)}$  is a diagonally dominant M-matrix. □

We now study various consequences of this characterization focusing on the Hüsler–Reiss precision matrix  $\Theta$  defined in (13). For a square matrix  $A$  denote by  $\text{Det}(A)$  its pseudo-determinant, that is, the product of all non-zero eigenvalues. The Weighted Matrix-Tree Theorem (Duval et al., 2009) gives the following.

**Lemma 4.4.** *If  $\Theta \in \mathbb{S}^d$  is such that  $\Theta \mathbf{1} = \mathbf{0}$  and  $Q_{ij} := -\Theta_{ij}$ ,  $i \neq j$ , then*

$$(16) \quad \text{Det}(\Theta) = d \cdot \sum_{T \in \mathcal{T}} \prod_{i,j \in T} Q_{ij},$$

where  $\mathcal{T}$  is the set of all spanning trees over the complete graph with vertices  $\{1, \dots, d\}$ . For any  $k = 1, \dots, d$  we have

$$(17) \quad \det(\Theta^{(k)}) = \sum_{T \in \mathcal{T}} \prod_{ij \in T} Q_{ij}.$$

We denote  $\mathbb{U}_+^d \subset \mathbb{S}^d$  to be the set of all graph Laplacians for connected graphs with positive weights on each edge. By Proposition 4.1,  $\Theta^{(k)}$  being a diagonally dominant M-matrix for one  $k \in [d]$  implies the same for all  $k \in [d]$ . In the next result we list equivalent conditions for that to happen.

**Lemma 4.5.** *Suppose that  $\Gamma$  is a strictly conditionally negative matrix. The following conditions are equivalent:*

- (i)  $\Theta_{ij} \leq 0$  for all  $i \neq j$ .
- (ii)  $\Theta \in \mathbb{U}_+^d$ , that is,  $\Theta$  is a Laplacian matrix of a connected graph with positive edge weights.
- (iii) For all  $k = 1, \dots, d$ ,  $\Theta^{(k)}$  is an M-matrix.
- (iv) For all  $k = 1, \dots, d$ ,  $\Theta^{(k)}$  is a diagonally dominant M-matrix.
- (v) For some  $k \in [d]$ ,  $\Theta^{(k)}$  is a diagonally dominant M-matrix.

*Proof.* (i) $\Rightarrow$ (ii) By Proposition 3.3, the row sums of  $\Theta$  are zero and  $\Theta_{ij} \leq 0$  for all  $i \neq j$ . It follows that  $\Theta$  is a Laplacian matrix of a graph weighted with  $Q_{ij} = -\Theta_{ij} \geq 0$ . Since  $\Gamma$  is strictly conditionally negative definite, again by Proposition 3.3,  $\text{rank}(\Theta) = d - 1$ . It then follows that  $\det(\Theta^{(k)}) > 0$ . By Lemma 4.4 we conclude that at least one of the tree terms is strictly positive proving that the underlying graph is connected, that is,  $\Theta \in \mathbb{U}_+^d$ .

(ii) $\Rightarrow$ (i) Follows immediately from the definition of a Laplacian matrix.

(i)  $\Leftrightarrow$  (iii) Clear because  $\Theta_{ij}^{(k)} = \Theta_{ij}$  for  $i, j$ .

(iii)  $\Leftrightarrow$  (iv) Clear because  $\Theta_{ij}^{(k)} = \Theta_{ij}$  for  $i, j$  and  $\Theta_{ii} = -\sum_{j \neq i} \Theta_{ij}$ , which implies that  $\sum_{j \neq k} \Theta_{ij}^{(k)} = -\Theta_{ik} \geq 0$ .

(iv)  $\Leftrightarrow$  (v) The left implication is clear. For the right implication, we argue as in the previous step. If  $\Theta^{(k)}$  is a diagonally dominant M-matrix then  $\Theta_{ij} \leq 0$  for all  $i, j \neq k$ . Similarly,  $\Theta_{ik} = -\sum_{j \neq k} \Theta_{ij}^{(k)} \leq 0$  (by diagonal dominance).  $\square$

As we noted in Appendix A.3, as long as  $\Gamma \in \mathcal{C}^d$ ,  $\sqrt{\Gamma_{ij}}$  are always distances in the sense that the map  $(i, j) \mapsto \sqrt{\Gamma_{ij}}$  is a metric function (satisfies the triangle inequality). In the special case when  $\Theta$  is a Laplacian matrix as in Lemma 4.5, the map  $(i, j) \mapsto \Gamma_{ij}$  is also a metric function by Lemma A.11. Although this result seems to be well known in the electrical network literature, the probabilistic interpretation that we present next is both new and illuminating.

**Proposition 4.6.** *A Hüsler–Reiss random vector is extremal associated if and only if its parameter matrix  $\Gamma$  satisfies the triangle inequality  $\Gamma_{ij} \leq \Gamma_{ik} + \Gamma_{jk}$  for all  $i, j, k \in [d]$ .*

*Proof.* First note that for a Hüsler–Reiss random vector  $\mathbf{Y}$ , it holds that  $\mathbf{Y}^k$  is associated if and only if  $\Sigma^{(k)}$  is non-negative. Indeed, by Proposition B.2(iv),  $\mathbf{Y}^k$  is associated if and only if  $\log \mathbf{Y}^k$  is associated. Note that, up to a simple adjustment of indices,  $\log \mathbf{Y}^k$  has an additive form as in Theorem 2.2 with  $X_0 = \log P$  and  $\mathbf{X} = (\log W_i^k)_{i \neq k}$ . Thus, by Theorem 2.2(3), we conclude that  $\log \mathbf{Y}^k$  is associated if and only if  $(\log W_i^k)_{i \neq k}$  is associated. Since  $(\log W_i^k)_{i \neq k}$  is Gaussian with covariance matrix  $\Sigma^{(k)}$  this is equivalent with  $\Sigma^{(k)} \geq 0$  by Proposition B.2(v).

Now the result follows from the fact that

$$\Sigma_{ij}^{(k)} \geq 0 \iff \Sigma_{ii}^{(k)} + \Sigma_{jj}^{(k)} \geq \Sigma_{ii}^{(k)} + \Sigma_{jj}^{(k)} - 2\Sigma_{ij}^{(k)} \iff \Gamma_{ik} + \Gamma_{jk} \geq \Gamma_{ij},$$

for all  $i, j, k \in [d]$ .  $\square$

This means that a Hüsler–Reiss distribution is extremal associated if and only if its parameter matrix  $\Gamma$  defines a metric. Since  $\text{MTP}_2$  always implies association (Karlin and Rinott, 1980, Corollary 4.1), if  $\mathbf{Y}$  is  $\text{EMTP}_2$  then it is extremal associated. In the electrical network literature, this corresponds to that statement that if  $\Theta$  is a Laplacian of a connected graph then the corresponding resistances  $\Gamma$  define a metric Fiedler (1998); Devriendt (2020); Klein and Randić (1993).

We now discuss the examples of bivariate and trivariate Hüsler–Reiss distributions with respect to Theorem 4.3 and Proposition 4.6.

**Example 2.** The bivariate Hüsler–Reiss distribution is generated from a log-Gaussian random variable with mean  $-\Gamma_{12}/2$  and variance  $\Gamma_{12}$ . Therefore, as  $\Theta^{(1)} = \Theta^{(2)} = 1/\Gamma_{12}$  is always positive by definition of  $\Gamma_{12}$ , it is always a diagonally dominant M-matrix and it follows that the bivariate Hüsler–Reiss distribution is  $\text{EMTP}_2$  for any  $\Gamma_{12}$ .

**Example 3.** Let  $d = 3$  and without loss of generality  $k = 3$ . Then,

$$\Sigma^{(3)} = \frac{1}{2} \begin{pmatrix} 2\Gamma_{13} & \Gamma_{13} + \Gamma_{23} - \Gamma_{12} \\ \Gamma_{13} + \Gamma_{23} - \Gamma_{12} & 2\Gamma_{23} \end{pmatrix}.$$

This means that

$$\Theta^{(3)} = \frac{2}{\det(\Sigma^{(3)})} \begin{pmatrix} 2\Gamma_{23} & -\Gamma_{13} - \Gamma_{23} + \Gamma_{12} \\ -\Gamma_{13} - \Gamma_{23} + \Gamma_{12} & 2\Gamma_{13} \end{pmatrix}.$$

The conditions in Theorem 4.3 translate to the triangle inequalities

$$(18) \quad \begin{aligned} \Gamma_{12} &\leq \Gamma_{13} + \Gamma_{23}, \\ \Gamma_{13} &\leq \Gamma_{12} + \Gamma_{23}, \\ \Gamma_{23} &\leq \Gamma_{12} + \Gamma_{13}, \end{aligned}$$

where the second and the third inequality come from the row sums. Note the symmetry in the inequalities, as  $\text{EMTP}_2$  does not depend on  $k$ . It follows that for trivariate Hüsler–Reiss distributions,  $\text{EMTP}_2$  and extremal association are equivalent. This resembles bivariate Gaussians, where association and  $\text{MTP}_2$  are equivalent.

**4.2. Other important constructions.** Another popular construction of multivariate Pareto distributions is when the extremal functions have the form

$$(19) \quad \mathbf{W}^k = (U_1/U_k, \dots, U_d/U_k),$$

for independent  $U_1, \dots, U_d$ . Examples include the extremal logistic (Tawn, 1990; Dombry et al., 2016) and the extremal Dirichlet distribution (Coles and Tawn, 1991), which we will discuss below.

Our next result provides a simple way of checking whether such constructions are  $\text{EMTP}_2$ .

**Proposition 4.7.** *Consider the multivariate Pareto distribution with stochastic representation (10). Suppose that  $W_i^k = U_i/U_k$  for some independent  $U_1, \dots, U_d$  such that  $\log U_i$  has a log-concave distribution for every  $i \in [d]$ . Then  $\mathbf{Y}$  is  $\text{EMTP}_2$ .*

*Proof.* By Theorem 4.2,  $\mathbf{Y}$  is  $\text{EMTP}_2$  if and only if  $(\log W_i^d)_{i \neq d} = (\log U_i - \log U_d)_{i \neq d}$  is strongly  $\text{MTP}_2$ . Let  $X_0 = -\log U_d$  and  $X_i = \log U_i$  for  $i = 1, \dots, d-1$ . Denoting  $\mathbf{X} = (X_1, \dots, X_{d-1})$ , the fact that  $\mathbf{X}$  is strongly  $\text{MTP}_2$  follows from Lemma 2.4, as the distribution of each  $X_i$  is log-concave. By assumption the distribution of  $-X_0$  is also log-concave and so the distribution of  $X_0$  must be log-concave. It follows from Theorem 2.2 that the vector  $(X_0, X_0 + X_1, \dots, X_0 + X_{d-1})$  is strongly  $\text{MTP}_2$ . Since the strong  $\text{MTP}_2$  property is closed under taking margins (Proposition 2.3) we conclude that

$$(X_0 + X_1, \dots, X_0 + X_{d-1}) = (\log U_1 - \log U_d, \dots, \log U_{d-1} - \log U_d)$$

is strongly  $\text{MTP}_2$ , proving that  $\mathbf{Y}$  is  $\text{EMTP}_2$ .  $\square$

From Proposition 4.7 it follows that both the extremal logistic and extremal Dirichlet distributions are always EMTP<sub>2</sub>.

**Example 4** (Extremal logistic distribution). The extremal logistic distribution with parameter  $\theta \in (0, 1)$  is defined by an extremal function  $\mathbf{W}^k$  as in (19) with  $U_i \sim \text{Fréchet}(1/\theta, G(1-\theta)^{-1})$  for  $i \neq k$  and  $(G(1-\theta)U_k)^{-1/\theta} := Z \sim \text{Gamma}(1-\theta, 1)$ , where  $G(x)$  is the Gamma function (Dombry et al., 2016). For  $i \neq k$ ,  $\log U_i$  follows a Gumbel distribution, which is log-concave. For  $i = k$ , observe

$$-\log(U_k) = \theta \log(Z) + \log(G(1-\theta)),$$

which means that  $-\log U_k \sim \text{ExpGamma}[1-\theta, \theta, \log(G(1-\theta))]$  follows an exponential Gamma distribution. An  $\text{ExpGamma}[\kappa, \theta, \mu]$  distribution has density

$$\frac{1}{\theta G(\kappa)} \exp\left(\frac{\kappa(x-\mu)}{\theta} - \exp\left(\frac{x-\mu}{\theta}\right)\right),$$

which is log-concave. Hence,  $\log U_k$  is log-concave by symmetry. By Proposition 19, this implies EMTP<sub>2</sub>.

**Example 5** (Extremal Dirichlet distribution). The extremal Dirichlet distribution with parameters  $\alpha_1, \dots, \alpha_d$  has an extremal function as in (19), where  $U_i \sim \text{Gamma}(\alpha_i, 1/\alpha_i)$  for  $i \neq k$  and  $U_k \sim \text{Gamma}(\alpha_k + 1, 1/\alpha_k)$  (Engelke and Volgushev, 2020). As the exponential Gamma distribution is log-concave, this is EMTP<sub>2</sub> by Proposition 4.7.

**4.3. Bivariate Pareto distributions and EMTP<sub>2</sub>.** A bivariate Pareto distribution  $\mathbf{Y} = (Y_1, Y_2)$  is completely characterized by a univariate distribution. Indeed, the extremal function then satisfies  $\mathbf{W}^1 = (1, W_2^1)$  with a positive random variable  $W_2^1$  with  $\mathbb{E}(W_2^1) = 1$ . The second extremal function  $\mathbf{W}^2 = (W_1^2, 1)$  is determined by the first one through the duality  $\mathbb{P}(W_1^2 \leq z) = \mathbb{E}(\mathbb{1}\{1/W_2^1\}W_2^1), z \geq 0$  (Engelke and Hitz, 2020, Example 3). Conversely, any positive random variable  $W_2^1$  with  $\mathbb{E}(W_2^1) = 1$  defines a unique bivariate Pareto distribution through the extremal function and duality.

These results extend to extremal tree models since they are a composition of bivariate Pareto distributions (Engelke and Volgushev, 2020); see Section 5.5.

By Theorem 4.2, EMTP<sub>2</sub> is equivalent to the univariate random variable  $W_2^1$  being strongly MTP<sub>2</sub>. This gives us the following result.

**Theorem 4.8.** *A bivariate Pareto distribution is EMTP<sub>2</sub> if and only if the distribution of  $\log W_2^1$  is log-concave. Furthermore, a bivariate Pareto distribution is always extremal associated.*

*Proof.* By Theorem 4.2, EMTP<sub>2</sub> is equivalent to  $\log W_2^1$  being strongly MTP<sub>2</sub>. But this is a univariate random variable so equivalently its density must be log-concave by Lemma 2.4.

By Proposition B.2(iv)  $\mathbf{Y}^k$  is associated if and only if  $\log \mathbf{Y}^k$  is associated. As univariate random variables are always associated (Proposition B.2(iii)), association follows from (10) and Theorem 2.2(3).  $\square$

Log-concave distributions include many known families like Gaussian, exponential, uniform, beta or Laplace, but also the class of generalized extreme value distributions, such that many bivariate Pareto distributions are indeed EMTP<sub>2</sub> for any parameter. The construction of an example where the bivariate Pareto distribution is not EMTP<sub>2</sub> requires a positive random variable  $W_2^1$  with mean 1 for which  $\log W_1^2$  is not log-concave. One example is when  $W_2^1$  is folded Laplace.

**Example 6.** Let  $W_2^1 = |X|$ , where  $X$  is distributed according to a Laplace distribution with mean  $\mu$  and scale parameter  $\sigma$ . The density of  $W_2^1$  equals

$$f(y) = \frac{1}{\sigma} \begin{cases} e^{-\mu/\sigma} \cosh(y/\sigma) & \text{for } 0 \leq y < \mu \\ e^{-y/\sigma} \cosh(\mu/\sigma) & \text{for } 0 \leq \mu \leq y \end{cases},$$

see also [Liu and Kozubowski \(2015\)](#). The density of  $\log W_2^1$  equals  $e^y f(e^y)$ , such that log-concavity of  $\log W_2^1$  requires that the second derivative of this is non-positive. We compute for  $0 \leq y < \mu$

$$\begin{aligned} \frac{\partial^2}{\partial y^2} \left( y - \log(\sigma) - \frac{\mu}{\sigma} + \log \cosh \left( \frac{e^y}{\sigma} \right) \right) &= \frac{\partial^2}{\partial y^2} \log \cosh \left( \frac{e^y}{\sigma} \right) \\ &= \frac{e^y \left( \sigma \tanh \left( \frac{e^y}{\sigma} \right) + e^y \operatorname{sech}^2 \left( \frac{e^y}{\sigma} \right) \right)}{\sigma^2}, \end{aligned}$$

which is clearly positive.

## 5. EMTP<sub>2</sub> IN GRAPHICAL EXTREMES

**5.1. Extremal conditional independence for multivariate Pareto distributions.** Let  $\mathbf{Y}$  be a multivariate Pareto random vector with support on the space  $\mathcal{L}$ . As mentioned above, the vector  $\mathbf{Y}^k$  is supported on a product space  $\mathcal{L}^k$ . The construction of  $\mathbf{Y}^k$  allows to define extremal conditional independence for multivariate Pareto distributions as follows:

**Definition 3.** ([Engelke and Hitz, 2020](#), Definition 5) Let  $A, B, C$  be disjoint subsets of  $[d]$ .  $\mathbf{Y}_A$  is extremal conditionally independent of  $\mathbf{Y}_B$  given  $\mathbf{Y}_C$  (abbreviated as  $\mathbf{Y}_A \perp_e \mathbf{Y}_B \mid \mathbf{Y}_C$ ) if for all  $k \in [d]$  it holds that

$$(20) \quad \mathbf{Y}_A^k \perp \mathbf{Y}_B^k \mid \mathbf{Y}_C^k.$$

It was shown that the condition in Definition 3 can be weakened ([Engelke and Hitz, 2020](#), Proposition 1) and, in fact, extremal conditional independence  $\mathbf{Y}_A \perp_e \mathbf{Y}_B \mid \mathbf{Y}_C$  already holds if there exists a  $k \in C$  in the conditioning set such that (20) is satisfied. Moreover, this is also equivalent to the factorization of the exponent measure density, that is,

$$\lambda(\mathbf{y}) = \frac{\lambda_{AC}(\mathbf{y}_{AC})\lambda_{BC}(\mathbf{y}_{BC})}{\lambda_C(\mathbf{y}_C)}, \quad \mathbf{y} \in \mathcal{E}.$$

Here and in the following, unions  $A \cup B$  of two sets  $A, B$  are abbreviated to  $AB$ .

**5.2. Graphical models for extremes.** Probabilistic graphical models encode conditional independence in graph structures. Let  $G = (V, E)$  be an undirected graph with vertex set  $V = [d]$  and edge set  $E$ . A random vector  $\mathbf{X}$  satisfies the pairwise Markov property with respect to  $G$ , when

$$X_i \perp X_j \mid \mathbf{X}_{\setminus ij}, \quad \text{if } (i, j) \notin E.$$

In this case, we call  $\mathbf{X}$  a *probabilistic graphical model*.

**Example 7.** For a multivariate Gaussian random vector  $\mathbf{X}$  with invertible covariance  $\Sigma$  and concentration matrix  $K = \Sigma^{-1}$ , it holds that  $X_i \perp X_j \mid \mathbf{X}_{\setminus ij}$  if and only if  $K_{ij} = 0$ . This means that for Gaussian graphical models, the concentration matrix contains the graph structure.

Definition 3 allows us to define graphical models that encode extremal conditional independence ([Engelke and Hitz, 2020](#), Section 4). Let  $G = (V, E)$  be an undirected graph with vertex set  $V$  and edge set  $E$ . A multivariate Pareto vector  $\mathbf{Y}$  satisfies the pairwise Markov property on  $\mathcal{L}$  with respect to  $G$  when

$$Y_i \perp_e Y_j \mid \mathbf{Y}_{\setminus ij}, \quad \text{if } (i, j) \notin E.$$

This means that  $Y_i$  and  $Y_j$  are extremal conditionally independent given all other variables if there is no edge between  $i$  and  $j$  in  $G$ . In fact, this resembles probabilistic graphical models, only with extremal conditional independence instead of standard conditional independence. In this case,  $\mathbf{Y}$  is called an extremal graphical model on  $G$ . For a decomposable graph  $G$  and if  $\mathbf{Y}$  has a positive and continuous density  $f_{\mathbf{Y}}$ , [Engelke and Hitz \(2020, Theorem 1\)](#) prove a Hammersley–Clifford theorem

showing the equivalence of the pairwise and global Markov properties, as well as a factorization of the density  $f_{\mathbf{Y}}$  with respect to  $G$ . Note that if  $\mathbf{Y}$  has a density then extremal graphical models are only defined for connected graphs [Engelke and Hitz \(2020, Remark 1\)](#), since marginal independence  $\mathbf{Y}_A \perp_e \mathbf{Y}_B$ ,  $A, B \subset V$  would contradict the existence of the density. This can be relaxed by dropping the assumption on existence of densities; see Kirstin Storkorb's discussion of [Engelke and Hitz \(2020\)](#).

**5.3. Axioms for conditional independence and faithfulness.** Conditional independence models can be discussed in a purely combinatorial way. We follow the definitions in [Fallat et al. \(2017, Section 5\)](#). Let  $\langle A, B \mid C \rangle$  be a ternary relation encoding abstract independence of  $A$  and  $B$  conditioning on  $C$ , where  $A, B, C$  are disjoint subsets of  $V$ . A conditional independence model  $\mathcal{I}$  is a set of such relations.  $\mathcal{I}$  is called a graphoid if it satisfies the following axioms for disjoint  $A, B, C, D \subset V$ :

- (1)  $\langle A, B \mid C \rangle \in \mathcal{I} \Leftrightarrow \langle B, A \mid C \rangle \in \mathcal{I}$  (symmetry),
- (2)  $\langle A, BD \mid C \rangle \in \mathcal{I} \Rightarrow \langle A, B \mid C \rangle \in \mathcal{I} \wedge \langle A, D \mid C \rangle \in \mathcal{I}$  (decomposition),
- (3)  $\langle A, BD \mid C \rangle \in \mathcal{I} \Rightarrow \langle A, B \mid CD \rangle \in \mathcal{I} \wedge \langle A, D \mid BC \rangle \in \mathcal{I}$  (weak union),
- (4)  $\langle A, B \mid CD \rangle \in \mathcal{I} \wedge \langle A, D \mid C \rangle \in \mathcal{I} \Leftrightarrow \langle A, BD \mid C \rangle \in \mathcal{I}$  (contraction),
- (5)  $\langle A, B \mid CD \rangle \in \mathcal{I} \wedge \langle A, C \mid BD \rangle \in \mathcal{I} \Rightarrow \langle A, BC \mid D \rangle \in \mathcal{I}$  (intersection).

A stochastic conditional independence model on a set of distributions is always a semi-graphoid, that is, it satisfies axioms (1)–(4). If in addition the distributions have positive densities, then it is a graphoid. In the discussion of [Engelke and Hitz \(2020\)](#), Steffen Lauritzen discusses that extremal conditional independence models are also semi-graphoids. Under the assumption of a positive exponent measure density  $\lambda$  that we make throughout the paper (see [Section 3.1](#)), the intersection axiom for extremal conditional independence for multivariate Pareto distributions follows from the fact that then, for any  $k \in V$ ,  $\mathbf{Y}^k$  satisfies the intersection axiom for classical stochastic conditional independence because its density is given by  $\lambda$ ; see [Pearl \(2009, Section 1.1.5\)](#) or [Lauritzen \(1996, Proposition 3.1\)](#).

For classical conditional independence, if the distributions are  $\text{MTP}_2$ , then [Fallat et al. \(2017\)](#) show that the following additional axioms are satisfied:

- (6)  $\langle A, B \mid C \rangle \in \mathcal{I} \wedge \langle A, D \mid C \rangle \in \mathcal{I} \Rightarrow \langle A, BD \mid C \rangle \in \mathcal{I}$  (composition),
- (7)  $\langle i, j \mid C \rangle \in \mathcal{I} \wedge \langle i, j \mid lC \rangle \in \mathcal{I} \Rightarrow \langle i, l \mid C \rangle \in \mathcal{I} \vee \langle j, l \mid C \rangle \in \mathcal{I}$  (singleton-transitivity),
- (8)  $\langle A, B \mid C \rangle \in \mathcal{I} \wedge D \subseteq V \setminus AB \Rightarrow \langle A, B \mid CD \rangle \in \mathcal{I}$  (upward-stability).

As a consequence, these axioms also hold for extremal conditional independence when the multivariate Pareto distribution is  $\text{EMTP}_2$ . In summary, we have the following theorem.

**Theorem 5.1.** *Extremal conditional independence for a multivariate Pareto distribution with positive density is a graphoid. If in addition the distribution is  $\text{EMTP}_2$ , then it is also upward-stable, singleton-transitive and compositional.*

We omit the proof since the statements follows from the corresponding statements for  $\mathbf{Y}^k$ ,  $k \in V$ . For extremal conditional independence on multivariate Pareto distributions with positive exponent measure density, we note that the following peculiarity arises. For instance, for  $D = \emptyset$ , the right-hand side of Axiom (5) would lead to unconditional independence  $A \perp_e BC$ , which is impossible as discussed in [Section 5.2](#). This is not a contradiction to the validity of Axiom (5), since it can be shown that in that case also the left-hand side can not arise.

**Remark 5.2.** Similar to conditional independence, extremal conditional independence under  $\text{EMTP}_2$  is equivalent to the respective collection of singleton conditional independences:

$$\mathbf{Y}_A \perp_e \mathbf{Y}_B \mid \mathbf{Y}_C \Leftrightarrow Y_i \perp_e Y_j \mid \mathbf{Y}_C \quad \forall i \in A, j \in B.$$

This follows as in [Lauritzen and Sadeghi \(2018, Corollary 1\)](#).

Many constraint-based structure learning algorithms, like the PC algorithm (Spirites et al., 2000) that is used to learn the skeleton in directed acyclic graphs, rely on the assumption that the dependence structure in the data-generating distribution reflects faithfully the graph. A distribution in a graphical model over a graph  $G$  is faithful if and only if each conditional independence corresponds exactly to graph separation. We define extremal faithfulness analogously.

For an undirected graph  $G = (V, E)$  we can define an independence model  $\mathcal{I}(G)$  through graph separation with respect to  $G$  by

$$\langle A, B \mid C \rangle \in \mathcal{I}(G) \iff C \text{ separates } A \text{ from } B,$$

where the latter means that all paths on  $G$  between  $A$  and  $B$  cross  $C$ . On the other hand, we can introduce an independence model  $\mathcal{I}_e(\mathbb{P}_{\mathbf{Y}})$  for a multivariate Pareto distributions  $\mathbf{Y}$  through

$$\langle A, B \mid C \rangle \in \mathcal{I}_e(\mathbb{P}_{\mathbf{Y}}) \iff \mathbf{Y}_A \perp_e \mathbf{Y}_B \mid \mathbf{Y}_C.$$

A multivariate Pareto distribution  $\mathbb{P}_{\mathbf{Y}}$  is said to be extremal faithful to a graph  $G$ , if  $\mathcal{I}_e(\mathbb{P}_{\mathbf{Y}}) = \mathcal{I}(G)$ .

**Theorem 5.3.** *Let  $\mathbf{Y}$  be a multivariate Pareto distribution with positive and continuous exponent measure that is an extremal graphical model on  $G$ . If  $\mathbf{Y}$  is in addition  $\text{EMTP}_2$ , then  $\mathcal{I}_e(\mathbb{P}_{\mathbf{Y}}) = \mathcal{I}(G)$ .*

The proof is similar to (Fallat et al., 2017, Theorem 6.1) who show that stochastic independence models that are  $\text{MTP}_2$  and satisfy the intersection axiom are always faithful to the corresponding pairwise independence graph. It is available in Appendix B.

We conclude Section 5.2 with two examples for extremal graphical models: Hüsler–Reiss graphical models and extremal tree models.

**5.4. Hüsler–Reiss graphical models.** It was shown in Engelke and Hitz (2020, Proposition 3) that extremal conditional independence for Hüsler–Reiss distributions can be read off from the inverse covariance matrix  $\Theta^{(k)} := (\Sigma^{(k)})^{-1}$ . Note that by construction, the extremal conditional independence does not depend on  $k$ , and this is also reflected by the relation between the  $\Theta^{(k)}$  for different  $k \in V$  (Engelke and Hitz, 2020, Lemma 1). Hentschel (2021) uses this to rephrase extremal conditional independence in terms of the Hüsler–Reiss precision matrix  $\Theta$  in (13), such that

$$(21) \quad Y_i \perp_e Y_j \mid \mathbf{Y}_{\setminus ij} \iff \Theta_{ij} = 0.$$

This equivalence shows the strong similarity of Hüsler–Reiss distributions with multivariate Gaussians, where conditional independences can equivalently be read off from the precision matrix.

We have seen that the Hüsler–Reiss distribution has many similar properties with respect to extremal conditional independence as the Gaussian distribution with respect to standard conditional independence. Therefore, Hüsler–Reiss graphical models are an analogue of Gaussian graphical models among extremal graphical models.

The following result corresponds to Proposition 6.3 in Fallat et al. (2017), which states that any undirected graph can be the concentration graph of an  $\text{MTP}_2$  Gaussian graphical model. We obtain the same statement for Hüsler–Reiss graphical models, with the intrinsic constraint for the graphs to be connected.

**Proposition 5.4.** *For every connected undirected graph  $G$  there exists an  $\text{EMTP}_2$  Hüsler–Reiss distribution that is Markov to  $G$ .*

*Proof.* Let  $\Theta$  be the Laplacian of  $G$  where each edge in  $G$  has edge weight 1. Clearly, the corresponding  $\Gamma$  is conditionally negative definite. By (21), a Hüsler–Reiss random vector with precision matrix  $\Theta$  is Markov to  $G$ , but by Lemma 4.5 it is also  $\text{EMTP}_2$ .  $\square$



**5.5. Extremal tree models.** For any undirected tree  $T = (V, E)$ , a multivariate Pareto distribution  $\mathbf{Y}$  that is Markov to  $T$  is called an extremal tree model (Engelke and Hitz, 2020). Such models also arise as the limits of regularly varying Markov trees (Segers, 2020). Define a directed tree  $T^k = (V, E^k)$  rooted in  $k$  by directing all edges in  $T$  away from  $k$ . By Engelke and Volgushev (2020, Proposition 1), for any  $k \in V$ , the extremal function  $\mathbf{W}^k$  has the stochastic representation

$$(22) \quad W_i^k = \prod_{e \in \text{ph}(ki; T^k)} W_e,$$

where  $\text{ph}(ki; T^k)$  is the set of directed edges on the path from  $k$  to  $i$  in  $T^k$  and  $\{W_e, e \in E^k\}$  is a set of independent random variables, where  $W_e$  with  $e = (i, j)$  has the distribution of  $W_j^i$ , that is, the  $j$ th component of the  $i$ th extremal function of  $\mathbf{Y}$ .

Let  $\mathbf{Y}$  be an arbitrary multivariate Pareto distribution. The extremal variogram rooted in node  $k$  is defined as

$$\Gamma^{(k)} = (\text{Var}(\log Y_i^k - \log Y_j^k))_{i,j \in V},$$

given that the variance exists. For an extremal tree model on the tree  $T$ , it was shown in Engelke and Volgushev (2020, Proposition 4) that the extremal variogram is a tree metric, that is,

$$\Gamma_{ij}^{(k)} = \sum_{mn \in \text{ph}(ij; T)} \Gamma_{mn}^{(k)}.$$

As a consequence, the minimum spanning tree with weights  $\Gamma_{ij}^{(k)} > 0$  is unique and equals the underlying tree  $T$  (Engelke and Volgushev, 2020, Corollary 1). The link of this model class to Brownian motion tree models is established in Proposition A.12 in Appendix A.

**Proposition 5.5.** *Extremal tree models are EMTP<sub>2</sub> if and only if all bivariate marginals are EMTP<sub>2</sub>, that is, if all  $\log W_e$  in (22) are log-concave. This implies that Hüsler–Reiss tree models are always EMTP<sub>2</sub>.*

*Proof.* By Theorem 4.2, we need to check whether  $(\log W_i^k)_{i \neq k}$  is strongly MTP<sub>2</sub>. By (22), it follows that

$$\log Y_i^k = \log P + \sum_{e \in \text{ph}(ki; T^k)} \log W_e,$$

where  $W_e, e \in E^k$  are independent. As  $\log P$  is log-concave, by Proposition 2.5 we have that  $\log \mathbf{Y}^k$  is strongly MTP<sub>2</sub> if and only if  $\log W_e$  is log-concave for each  $e \in E$ . This is equivalent to  $(\log W_i^k)_{i \neq k}$  being strongly MTP<sub>2</sub> by Theorem 2.2(2). From Example 2 it then follows that Hüsler–Reiss tree models are always EMTP<sub>2</sub>.  $\square$

In comparison, Gaussian tree models are MTP<sub>2</sub> if and only if their covariance is non-negative, that is, if they are associated (Lauritzen et al., 2019, Proposition 5.3). This is one way to illustrate why EMTP<sub>2</sub> constraints are more natural for extreme data than MTP<sub>2</sub> constraints are in the classical case.

**Remark 5.6.** Note that as univariate random variables are associated, the construction in the proof of Proposition 2.5 would indicate that  $\log \mathbf{Y}^k$  is associated even when  $\log W_e$  is not log-concave. As a consequence, any extremal tree model should be extremal associated.

## 6. LEARNING TOTALLY POSITIVE HÜSLER–REISS GRAPHICAL MODELS

The work of [Slawski and Hein \(2015\)](#) and [Lauritzen et al. \(2019\)](#) shows that in the Gaussian case, the MLE under  $\text{MTP}_2$  has many nice properties. For example, the maximum likelihood estimator exists with probability 1 as long as the sample size is at least two and the  $\text{MTP}_2$  constraint works as an implicit regularizer. In this section, we study the estimation of Hüsler–Reiss distributions under the  $\text{EMTP}_2$  constraint replacing the likelihood function with a surrogate likelihood.

**6.1. Surrogate likelihood and its dual.** In order to use properties of Gaussian maximum likelihood theory we apply a transformation to a Hüsler–Reiss Pareto distribution  $\mathbf{Y}$ . Recall that  $\mathbf{Y}^k$  is defined as the conditioned random vector  $\mathbf{Y} \mid Y_k > 1$  and that from Section 3.2 we have for a Hüsler–Reiss distribution with parameter matrix  $\Gamma \in \mathcal{C}^d$

$$(23) \quad (\log Y_i^k - \log Y_k^k)_{i \neq k} = \log \mathbf{W}_{\setminus k}^k \sim N(-\text{diag}(\Sigma^{(k)})/2, \Sigma^{(k)}).$$

Consider a data matrix  $y \in \mathbb{R}^{n \times d}$  of  $n$  independent observations of  $\mathbf{Y}$  with  $i$ th row  $(y_{i1}, \dots, y_{id})$ . Let  $\mathcal{I}_k = \{i \in [n] : y_{ik} > 1\}$  be the index set of observations where the  $k$ th coordinate exceeds one. If  $|\mathcal{I}_k| \geq 2$ , for any  $i \in \mathcal{I}_k$ ,  $k \in [d]$ , we define independent observations  $\mathbf{w}_i$  of  $\mathbf{W}^k$  by

$$w_{ij} = \log y_{ij} - \log y_{ik}, \quad j = 1, \dots, d,$$

and let the corresponding sample covariance matrix be

$$(24) \quad \Omega^{(k)} = \frac{1}{|\mathcal{I}_k|} \sum_{i \in \mathcal{I}_k} (\mathbf{w}_i - \bar{\mathbf{w}})(\mathbf{w}_i - \bar{\mathbf{w}})^T, \quad \text{where } \bar{\mathbf{w}} = \frac{1}{|\mathcal{I}_k|} \sum_{i \in \mathcal{I}_k} \mathbf{w}_i.$$

Note that, by construction,  $w_{ik} = 0$  for all  $i \in \mathcal{I}_k$  and so the  $k$ th row/column of  $\Omega^{(k)}$  is zero. If  $|\mathcal{I}_k| < 2$ , set  $\Omega^{(k)} = 0$ . We obtain the empirical variogram  $\bar{\Gamma}^{(k)}$  from  $\Omega^{(k)}$  via the inverse Farris transform

$$(25) \quad \bar{\Gamma}_{ij}^{(k)} = \Omega_{ii}^{(k)} + \Omega_{jj}^{(k)} - 2\Omega_{ij}^{(k)} \quad \text{for all } i, j.$$

Because the index set  $\mathcal{I}_k$  depends on  $k$ , the estimator  $\bar{\Gamma}^{(k)}$  also depends on  $k$ . In order to obtain an estimate of  $\Gamma$  that is symmetric and uses all data, we define the combined empirical variogram as

$$(26) \quad \bar{\Gamma} := \frac{1}{d} \sum_{k=1}^d \bar{\Gamma}^{(k)};$$

see also [Engelke and Volgushev \(2020, Corollary 2\)](#). For each  $k = 1, \dots, d$ , via the Farris transform (11), we obtain an empirical covariance  $S^{(k)}$  from  $\bar{\Gamma}$ .

The inverse covariance matrix of  $\log \mathbf{W}_{\setminus k}^k$  can be estimated by maximizing the surrogate log-likelihood that takes the form

$$(27) \quad \ell(\Theta^{(k)}; S^{(k)}) := \log \det \Theta^{(k)} - \text{tr}(S^{(k)} \Theta^{(k)}),$$

which is derived from (23) by dropping the likelihood contribution of the mean vector  $-\text{diag}(\Sigma^{(k)})/2$ . Maximizing this would result in an estimate of  $\Theta^{(k)}$  that is close to the maximum likelihood estimator since the mean vector only contains information on the diagonal of  $\Sigma^{(k)}$ . Note that the function  $\ell(\Theta^{(k)}; S^{(k)})$  in (27) is directly related to the log-determinantal Bregman divergence (e.g., [Ravikumar et al., 2011](#)).

A more elegant formulation of the surrogate log-likelihood that is independent of  $k$  is given in the next lemma. As in Appendix A, if  $\Theta \in \mathbb{U}$  then  $Q \in \mathbb{S}_0^d$  is defined by  $Q_{ij} = -\Theta_{ij}$ . Moreover, we equip  $\mathbb{S}_0^d$  with the inner product  $\langle\langle A, B \rangle\rangle := \sum_{i < j} A_{ij} B_{ij}$ .

**Lemma 6.1.** *The right-hand side of (27) can be rewritten in terms of  $\Theta$  as*

$$(28) \quad \ell(\Theta, S) = \log \det \Theta - \langle S, \Theta \rangle - \log(d),$$

where  $S = \mathbf{P}(-\frac{1}{2}\bar{\Gamma})\mathbf{P}$  with  $\mathbf{P}$  defined in (14), or, equivalently, in terms of  $Q \in \mathbb{S}_0^d$  as

$$(29) \quad \ell(Q; \bar{\Gamma}) = \log\left(\sum_{T \in \mathcal{T}} \prod_{ij \in T} Q_{ij}\right) - \langle \bar{\Gamma}, Q \rangle.$$

*Proof.* We use the notation of Appendix A, where  $\tilde{S}^{(k)}$  is embedding  $S^{(k)} \in \mathbb{S}^{d-1}$  in  $\mathbb{S}^d$  by adding to it a zero row/column (as the  $k$ th row/column). Similarly  $\tilde{\Theta}^{(k)}$  is the pseudoinverse of  $\tilde{S}^{(k)}$ . Note that  $\langle S^{(k)}, \Theta^{(k)} \rangle = \langle \tilde{S}^{(k)}, \tilde{\Theta}^{(k)} \rangle$ , which is equal to  $\langle \bar{\Gamma}, Q \rangle$  simply because both are equal to  $\langle \bar{\Gamma}, Q \rangle$  by Remark A.1(4). This gives

$$\langle S^{(k)}, \Theta^{(k)} \rangle = \langle S, \Theta \rangle = \langle \bar{\Gamma}, Q \rangle.$$

Moreover, by Lemma 4.4,

$$\log \det \Theta^{(k)} = \log\left(\sum_{T \in \mathcal{T}} \prod_{ij \in T} Q_{ij}\right) = \log \det \Theta - \log(d).$$

This proves both (28) and (29).  $\square$

In order to enforce the EMTP<sub>2</sub> constraint for the Hüsler–Reiss distribution, we propose to solve a restricted optimization problem using the characterization in Theorem 4.3 and Lemma 4.5. Recall that  $\mathbb{U}_+^d \subset \mathbb{S}^d$  denotes the set of all graph Laplacians for connected graphs with positive weights on each edge. Slightly abusing notation, we also denote by  $\mathbb{U}_+$  its image in  $\mathbb{S}_0$ , that is, the points in the nonnegative orthant of  $\mathbb{S}_0$  whose support is a connected graph. Thus, for any fixed  $\bar{\Gamma}$  we consider the problem of maximizing  $\ell(Q; \bar{\Gamma})$  in (29) over  $\mathbb{U}_+$ , that is,

$$(30) \quad \hat{Q} := \arg \max_{Q \in \mathbb{U}_+} \ell(Q; \bar{\Gamma}).$$

This is a convex optimization problem because  $\ell(Q; \bar{\Gamma})$  is a strictly concave function over the convex set  $\mathbb{U}_+$ .

We call  $\hat{Q}$  a surrogate maximum likelihood estimator for  $Q$  under EMTP<sub>2</sub>. To obtain an estimator  $\hat{\Gamma}$  for the variogram under EMTP<sub>2</sub>, we first take  $\hat{\Theta}$  given by  $\hat{\Theta} = -\hat{Q}_{ij}$  to define  $\hat{\Sigma} = \hat{\Theta}^+$  and then map

$$\hat{\Gamma}_{ij} = \hat{\Sigma}_{ii} + \hat{\Sigma}_{jj} - 2\hat{\Sigma}_{ij}$$

as explained in Appendix A. This is not the maximum likelihood estimator of  $\Gamma$  under the EMTP<sub>2</sub> constraint because we have dropped the contribution of the mean vector as in (27). Nevertheless,  $\hat{\Gamma}$  is a very natural estimator since it has a simple interpretation in terms of the input matrix  $\bar{\Gamma}$ ; see Theorem 6.3 below. Moreover, we show in Proposition 6.6 that it is a consistent estimator.

To analyze this optimization problem in more detail, we study it from the perspective of convex analysis. We first derive its dual problem.

**Proposition 6.2.** *The dual problem of (30) is:*

$$(31) \quad \text{maximize } \log \det \begin{pmatrix} 0 & -\mathbf{1}^T \\ \mathbf{1} & -\frac{1}{2}\bar{\Gamma} \end{pmatrix} + (d-1) \quad \text{subject to } \Gamma \in \mathcal{C}^d \text{ and } \Gamma \leq \bar{\Gamma}.$$

*Proof.* Let  $\mathcal{K}^d$  be the set of all  $Q \in \mathbb{S}_0^d$  such that the corresponding  $\Gamma$  lies in  $\mathcal{C}^d$ . For given  $\bar{\Gamma}$  we define the extended-real-valued function

$$(32) \quad f(Q) = \begin{cases} -\ell(Q; \bar{\Gamma}) & \text{if } Q \in \mathcal{K}^d \\ +\infty & \text{otherwise.} \end{cases}$$

The problem in (30) can be therefore reformulated as follows:

$$(33) \quad \text{minimize } f(Q) \quad \text{subject to } Q \geq 0.$$

The Lagrangian for this problem is  $f(Q) - \langle \Lambda, Q \rangle$ , where  $\Lambda \in \mathbb{S}_0^d$  and  $\Lambda_{ij} \geq 0$  for all  $1 \leq i < j \leq d$  (Lagrange multipliers of the non-negative constraints). Clearly,

$$\sup_{\Lambda \geq 0} \{f(Q) - \langle \Lambda, Q \rangle\} = \begin{cases} f(Q) & \text{if } Q \geq 0, \\ +\infty & \text{otherwise.} \end{cases}$$

This implies that Problem (33) is equivalent to

$$\inf_Q \sup_{\Lambda \geq 0} \{f(Q) - \langle \Lambda, Q \rangle\}$$

where the infimum is unrestricted. By duality theory (Slater's conditions), we obtain the same value by swapping inf and sup. We obtain the Lagrange dual function

$$\inf_Q \{f(Q) - \langle \Lambda, Q \rangle\}.$$

If the infimum exists, it is obtained at the unique  $Q \in \mathcal{K}^d$  for which the gradient of  $f(Q) - \langle \Lambda, Q \rangle$  vanishes. By Proposition A.5,

$$\nabla_Q \log\left(\sum_{T \in \mathcal{T}} \prod_{ij \in T} Q_{ij}\right) = \Gamma$$

and so

$$\nabla \{f(Q) - \langle \Lambda, Q \rangle\} = -\Gamma + \bar{\Gamma} - \Lambda$$

showing that the optimal point must satisfy  $\Gamma \leq \bar{\Gamma}$  and  $\Lambda = \bar{\Gamma} - \Gamma$  and so optimizing the dual function is equivalent to optimizing a function of  $\Gamma$  of the form

$$(34) \quad h(\Gamma) = \begin{cases} \log \det(\Sigma^{(k)}(\Gamma)) + (d-1) & \text{if } \Gamma \leq \bar{\Gamma}, \Gamma \in \mathcal{C}^d, \\ -\infty & \text{otherwise.} \end{cases}$$

Finally, we use the Cayley–Menger formula that states that for every  $k = 1, \dots, d$

$$(35) \quad \det(\Sigma^{(k)}) = \det \begin{pmatrix} 0 & -\mathbf{1}^T \\ \mathbf{1} & -\frac{1}{2}\Gamma \end{pmatrix}.$$

□

The proof of the previous result and the KKT conditions imply the following result.

**Theorem 6.3.** *The point  $(\hat{Q}, \hat{\Gamma})$  is the unique optimal point of  $f(Q)$  over  $Q \in \mathbb{U}_+$  if and only if:*

- (i)  $\hat{Q}_{ij} \geq 0$  for all  $1 \leq i < j \leq d$ ,
- (ii)  $\bar{\Gamma}_{ij} \geq \hat{\Gamma}_{ij}$  for all  $1 \leq i < j \leq d$ ,
- (iii)  $(\bar{\Gamma}_{ij} - \hat{\Gamma}_{ij})\hat{Q}_{ij} = 0$  for all  $1 \leq i < j \leq d$ .

**6.2. Existence of the optimum and its consistency.** Lemma 4.5 and Lemma 6.1 show that optimizing (27) with respect to all diagonally dominant M-matrices  $\Theta^{(k)}$  is equivalent to optimizing  $-\log \text{Det } \Theta + \langle S, \Theta \rangle$  over all Laplacian matrices  $\Theta$  of connected graphs, as described in (30). This is precisely the optimization problem considered in Equation (3) in Ying et al. (2021). They show in Theorem 1 that the optimum in (30) exists almost surely. The proof of this result in the supplement of Ying et al. (2021) actually reveals a more detailed statement, which is useful for our purposes:

**Theorem 6.4.** *The optimum of the problem (30) exists if and only if  $\bar{\Gamma}_{ij} > 0$  for all  $1 \leq i < j \leq d$ .*

We provide our own proof of this result, which uses the dual problem, in Appendix B.

Note that  $\bar{\Gamma}_{ij} = 0$  if and only if  $\bar{\Gamma}_{ij}^{(k)} = 0$  for all  $k$ ; see (26). Moreover,  $\bar{\Gamma}_{ij}^{(k)} = 0$  if and only if  $\Omega_{ii}^{(k)} = \Omega_{ij}^{(k)} = \Omega_{jj}^{(k)}$ . This happens with probability zero with respect to the underlying sample unless the corresponding index set  $\mathcal{I}_k$  satisfies  $|\mathcal{I}_k| < 2$ . Thus, with probability one,  $\bar{\Gamma}_{ij} > 0$  unless for each  $k \in [d]$  the event  $\{Y_k > 1\}$  is observed at most once in the sample.

We finish this section providing a consistency result that uses consistency of  $\bar{\Gamma}$  and the Berge's maximum theorem (see Berge, 1997, Section VI.3).

**Proposition 6.5.** *The function*

$$\bar{\Gamma} \mapsto \hat{\Gamma} = \operatorname{argmax}_{\Gamma \in \mathcal{C}^d \cap \{\Gamma \leq \bar{\Gamma}\}} \log \det \begin{pmatrix} 0 & -\mathbf{1}^T \\ \mathbf{1} & -\frac{1}{2}\Gamma \end{pmatrix}$$

*is a continuous function over all  $\bar{\Gamma}$  such that  $\bar{\Gamma}_{ij} > 0$  for all  $i \neq j$ .*

*Proof.* Consider the function  $f : \mathcal{C}^d \rightarrow \mathbb{R}$  given by

$$f(\Gamma) := \log \det \begin{pmatrix} 0 & -\mathbf{1}^T \\ \mathbf{1} & -\frac{1}{2}\Gamma \end{pmatrix}.$$

This function is indeed well-defined by the Cayley–Menger formula in (35) and Lemma 3.2. If  $\bar{\Gamma}_{ij} > 0$  for all  $i \neq j$  then the set of all  $\Gamma \in \mathcal{C}^d$  satisfying  $\Gamma \leq \bar{\Gamma}$  (for a fixed  $\bar{\Gamma}$ ) is a bounded non-empty set. Since  $\Gamma_{ij} > 0$  for all  $i < j$ , by Proposition 6.4, there is a unique point in this set that maximizes  $f(\Gamma)$  which shows that the  $\operatorname{argmax}$  mapping in the statement is indeed a well-defined function. Moreover, by strict concavity of  $f(\Gamma)$ , the same holds if we maximize  $f$  over the closure of  $\mathcal{C}^d \cap \{\Gamma \leq \bar{\Gamma}\}$ . This is a compact set, which we denote by  $g(\bar{\Gamma}) := \bar{\mathcal{C}}^d \cap \{\Gamma \leq \bar{\Gamma}\}$ , where  $\bar{\mathcal{C}}^d$  is the closure of  $\mathcal{C}^d$ . Consider the set  $\mathcal{K}$  of all compact subsets in  $\mathbb{S}_0^d$ . This set forms a metric space with the Hausdorff distance

$$\mathbb{D}(C, D) := \max \left\{ \max_{\Gamma \in C} d_D(\Gamma), \max_{\Gamma \in D} d_C(\Gamma) \right\}, \quad C, D \in \mathcal{K},$$

where  $d_C(\Gamma)$  denotes the Euclidean distance of  $\Gamma \in \mathbb{S}_0^d$  to the set  $C \in \mathcal{K}$ . The mapping  $g : \mathbb{S}_0^d \rightarrow \mathcal{K}$  defined as above is a mapping between two metric spaces. This map is continuous if and only if for every sequence if  $\Gamma_n \rightarrow \bar{\Gamma}$  then  $g(\Gamma_n) \rightarrow g(\bar{\Gamma})$ . Equivalently, we want to show that

$$(36) \quad \|\Gamma_n - \bar{\Gamma}\| \rightarrow 0 \implies \mathbb{D}(g(\Gamma_n), g(\bar{\Gamma})) \rightarrow 0.$$

Let  $C_n = g(\Gamma_n)$  and  $D = g(\bar{\Gamma})$ . Since  $\bar{\Gamma}$  is an interior point of  $\mathcal{C}^d$ , we can assume that  $\Gamma_n \in \mathcal{C}^d$  as well. But for every  $\Gamma \in \bar{\mathcal{C}}^d$

$$d_D(\Gamma) = \sqrt{\sum_{i < j} (\max\{(\Gamma - \bar{\Gamma})_{ij}, 0\})^2} \leq \sqrt{\sum_{i < j} (\Gamma - \bar{\Gamma})_{ij}^2} = \|\Gamma - \bar{\Gamma}\|.$$

The same argument shows that for every  $\Gamma \in C_n$  we have  $d_D(\Gamma) \leq d_D(\Gamma_n)$  and so

$$\max_{\Gamma \in C_n} d_D(\Gamma) = d_D(\Gamma_n) \leq \|\Gamma_n - \bar{\Gamma}\|.$$

By symmetry we can also show that  $\max_{\Gamma \in D} d_{C_n}(\Gamma) \leq \|\Gamma_n - \bar{\Gamma}\|$ , which implies

$$\mathbb{D}(g(\Gamma_n), g(\bar{\Gamma})) \leq \|\Gamma_n - \bar{\Gamma}\|,$$

and thus also (36). We have established continuity of  $g$ . By the Maximum Theorem in Berge (1997, Section VI.3), the function  $\bar{\Gamma} \mapsto \operatorname{argmax}_{\Gamma \in g(\bar{\Gamma})} f(\Gamma)$  is also continuous.  $\square$

As a consequence we establish the consistency of the estimator  $\hat{\Theta}$  under EMTP<sub>2</sub>.

**Theorem 6.6.** *Let  $\mathbf{Y}$  be a multivariate Pareto distribution with parameter matrix  $\Gamma$  such that the corresponding precision matrix  $\Theta \in \mathbb{U}_+^d$  is Laplacian. Then, the EMTP<sub>2</sub> estimator  $\hat{\Gamma}$  based on  $n$  independent samples of  $\mathbf{Y}$  is consistent for  $n \rightarrow \infty$ .*

*Proof.* By Engelke and Volgushev (2020, Theorem 1),  $\bar{\Gamma}$  converges weakly to the true  $\Gamma$ . Moreover,  $\hat{\Gamma}$  is a continuous function of  $\bar{\Gamma}$  by Proposition 6.5. It follows that  $\hat{\Gamma}$  converges weakly to the true  $\Gamma$ .  $\square$

## 7. AN OPTIMIZATION ALGORITHM

Our aim in this section is to develop a numerical algorithm to optimize the surrogate likelihood in (28) in terms of  $\Theta$  (equiv. (29) in terms of  $Q$ ). A natural first idea is a projected coordinate descent algorithm as both the gradient of this function has a simple form and the projection on the set  $\Theta \leq 0$  is straightforward. This is precisely the algorithm proposed in Ying et al. (2021). We note however that ensuring that at each iteration  $\Theta$  is a Laplacian of a *connected* graph is harder and it occasionally leads to numerical issues.

In what follows we develop a block coordinate descent algorithm that optimizes the dual problem updating  $\Gamma$  row by row. This algorithm carefully exploits the structure of the problem and relies on quadratic programming. Although in our setting  $S$  that appears in (28) is a positive semi-definite matrix satisfying  $S\mathbf{1} = \mathbf{0}$ , our algorithm takes as input *any* positive semi-definite matrix satisfying  $S_{ii} > 0$  for all  $i \in [d]$  and  $S_{ij} < \sqrt{S_{ii}S_{jj}}$  for all  $i \neq j$ . We observe that our algorithm is more stable than the projected gradient descent algorithm in the case when  $S$  is rank deficient.

**7.1. General description of the algorithm.** Our algorithm is a block coordinate descent algorithm that optimizes the dual problem (31). We refer to all  $\Gamma \in \mathcal{C}^d$  satisfying  $\Gamma \leq \bar{\Gamma}$  as the dually feasible points. The algorithm starts at some given dually feasible point and it updates the  $\Gamma$  matrix row by row. At each step the value of the function increases and the corresponding point is dually feasible. Updating a row requires solving a quadratic problem. This is similar to the algorithms used for the graphical LASSO (Banerjee et al., 2008; Lauritzen and Zwiernik, 2020b) but with important twists.

Denote  $A = -\frac{1}{2}\Gamma$  and assume  $d \geq 3$ . After suitably reordering the rows/columns of  $A$ , for any  $i = 1, \dots, d$ , we can rewrite the determinant in (31) as

$$(37) \quad -\det \begin{bmatrix} 0 & 1 & \mathbf{1}^T \\ 1 & 0 & A_{\setminus i, i}^T \\ \mathbf{1} & A_{\setminus i, i} & A_{\setminus i, \setminus i} \end{bmatrix}.$$

The goal in the dual problem (31) is to optimize this expression subject to  $\Gamma \leq \bar{\Gamma}$ . Instead, we optimize this expression only with respect to  $\mathbf{y} = A_{\setminus i, i}$ . This will lead to a quadratic optimization problem that we can easily solve.

Let  $B = (A_{\setminus i, \setminus i})^{-1}$ . Since  $\Gamma \in \mathcal{C}^d$ , also  $\Gamma_{\setminus i, \setminus i} \in \mathcal{C}^{d-1}$  and, in particular,  $\mathbf{1}^T \Gamma_{\setminus i, \setminus i} \mathbf{1} > 0$ . In consequence, by Micchelli (1986, Lemma 3.2),  $\Gamma_{\setminus i, \setminus i}$  has  $d-2$  negative eigenvalues and one positive eigenvalue. Hence,

$$\det(A_{\setminus i, \setminus i}) = \frac{1}{(-2)^{d-1}} \det(\Gamma_{\setminus i, \setminus i}) < 0.$$

Using the standard Schur complement arguments, (37) can be written as

$$-\det(A_{\setminus i, \setminus i}) \cdot \left( \mathbf{y}^T (\mathbf{1}^T B \mathbf{1} B - B \mathbf{1} \mathbf{1}^T B) \mathbf{y} + 2 \mathbf{1}^T B \mathbf{y} - 1 \right),$$

which has to be maximized with respect to  $\mathbf{y}$ . Thus, equivalently, to maximize the expression in (37) with respect to  $\mathbf{y}$ , we minimize the quadratic function

$$(38) \quad \mathbf{y}^T (B \mathbf{1} \mathbf{1}^T B - \mathbf{1}^T B \mathbf{1} B) \mathbf{y} - 2 \mathbf{1}^T B \mathbf{y},$$

subject to  $\mathbf{y} \geq -\frac{1}{2}\bar{\Gamma}_{\setminus i, i}$ . This is a simple quadratic optimization problem. However, an important complication comes from the fact that the corresponding quadratic form is not positive definite (it contains the vector of ones in its kernel) and so many of the popular quadratic programming algorithms cannot be used. In our calculations we have used the `OSQP` package in R (Stellato et al., 2020).

In summary, our algorithm relies on a sequence of simple quadratic optimization problems and it is outlined below. An implementation of this algorithm is available as the `emtp2` function of the R package `graphicalExtremes` (Engelke et al., 2020).

**Data:** Conditionally negative definite  $\bar{\Gamma}$ .

**Result:** A maximizer of (31).

Initialize:  $\Gamma = \Gamma^0$  (a dually feasible point; see Section 7.3);

**while** *there is no convergence* **do**

**for**  $i = 1, \dots, d$  **do**

        Update  $\Gamma_{i, \setminus i} \leftarrow -2\hat{\mathbf{y}}$ , where  $\hat{\mathbf{y}}$  is the minimizer of (38) subject to  $\mathbf{y} \geq -\frac{1}{2}\bar{\Gamma}_{\setminus i, i}$ .

**end**

**end**

**Algorithm 1:** The block coordinate descent algorithm for Hüsler–Reiss distributions under EMTP<sub>2</sub>.

The fact that each iteration gives a dually feasible point will be now proven formally.

**Proposition 7.1.** *Each iteration of Algorithm 1 is a dually feasible point.*

*Proof.* Since the starting point  $\Gamma^0$  is an arbitrary dually feasible point, it is enough to show that updating its  $i$ th row/column gives a dually feasible point. The constraint  $\Gamma \leq \bar{\Gamma}$  is embedded explicitly in the optimization problem so it is clearly satisfied. To argue that  $\Gamma \in \mathcal{C}^d$  (which is not explicitly imposed), note that  $\Gamma$  is obtained by maximizing

$$(39) \quad \det \begin{pmatrix} 0 & -\mathbf{1}^T \\ \mathbf{1} & -\frac{1}{2}\Gamma \end{pmatrix},$$

which by the Cayley–Menger formula in (35) is equal to the determinant of  $\Sigma^{(k)}$  for every  $k \in [d]$ . Suppose that the algorithm updates the  $i$ th row/column of  $\Gamma$  and fix any  $k \neq i$ . By Lemma A.8,  $\Gamma \in \mathcal{C}^d$  if and only if  $\Sigma^{(k)}$  is positive definite. Using Sylvester’s criterion, equivalently  $\det(\Sigma_B^{(k)}) > 0$  for every nonempty  $B \subseteq [d] \setminus \{i, k\}$  and  $B = [d] \setminus \{k\}$  (enough to check the leading principal minors when the rows of  $\Sigma_B^{(k)}$  are arranged so that the  $i$ th row/column comes last). By (11),  $\Sigma_B^{(k)}$  is an explicit linear function of  $\Gamma_{B \cup \{k\}}$ . Using the Cayley–Menger formula again we get

$$(40) \quad \det(\Sigma_B^{(k)}) = \det \begin{pmatrix} 0 & -\mathbf{1}^T \\ \mathbf{1} & -\frac{1}{2}\Gamma_{B \cup \{k\}} \end{pmatrix}.$$

If  $B \subseteq [d] \setminus \{i, k\}$  then the update of the algorithm does not affect this quantity and so  $\det(\Sigma_B^{(k)}) > 0$  by the fact that the current estimate was dually feasible. If  $B = [d] \setminus \{k\}$  then the right hand side of (40) becomes (39). This quantity must then be strictly positive after the update because it is at least as big as for the current estimate, which was strictly positive.  $\square$

**7.2. Convergence criteria.** Recall that by strong duality we can guarantee that at the optimal point  $(\Gamma^*, Q^*)$  the value of the primal and the dual functions are equal and for any other point the value of the dual problem is lower. Thus, to obtain a convergence criterion it is natural to track the duality gap

$$(41) \quad -\log \det \Theta^{(k)} + \langle \bar{\Gamma}, Q \rangle - (\log \det \Sigma^{(k)} + (d-1)) = \langle \bar{\Gamma}, Q \rangle - (d-1),$$



which is guaranteed to be always nonnegative and zero precisely at the optimal point. The algorithm may be stopped when the duality gap is lower than some fixed threshold. Optimality of the obtained point can be verified using the KKT conditions in Theorem 6.3. Note however that, to compute the duality gap, the current estimate  $\Gamma$  needs to be mapped to  $Q$ . This operation involves pseudo-inversion and so it may be expensive in high-dimensional situations. In this case, we can simply track the absolute change between the updates of  $\Gamma$  checking the duality gap only in the end to decide if more iterations are needed.

**7.3. A starting point.** For our coordinate descent algorithm to work, we require a feasible starting point. By Proposition 7.1, every subsequent point in our procedure will be dually feasible. Our construction relies on ideas that were used in the context of Gaussian distributions. Let  $S$  be a positive semi-definite matrix. By Proposition 3.4 in Lauritzen et al. (2019), as long as  $S_{ii} > 0$  for all  $i = 1, \dots, d$  and  $S_{ij} < \sqrt{S_{ii}S_{jj}}$  for all  $i \neq j$ , there exists a positive definite matrix  $Z$  such that  $Z \geq S$  and  $Z$  coincides with  $S$  on the diagonal. The construction of such  $Z$  links to single-linkage clustering and ultrametrics. Section 3 in Lauritzen et al. (2019) also describes an efficient method for computing  $Z$ , which is implemented as function `Zmatrix` in the R package `golazo` (Lauritzen and Zwiernik, 2020a). Let  $\Gamma^Z$  be obtained from  $Z$  via the inverse Farris transform. Note that by construction  $\Gamma^Z$  is strictly conditionally negative definite and

$$\Gamma_{ij}^Z = Z_{ii} + Z_{jj} - 2Z_{ij} = S_{ii} + S_{jj} - 2Z_{ij} \leq S_{ii} + S_{jj} - 2S_{ij} = \bar{\Gamma}_{ij}.$$

As a consequence,  $\Gamma^Z$  is a valid starting point for our block coordinate descent algorithm.

**7.4. Performance.** In our setup, the optimization of (30) arises naturally as the EMTP<sub>2</sub> constraint maximization of the surrogate likelihood of the Hüsler–Reiss distribution. The same optimization problem appears in the literature on graph learning under Laplacian constraints (Egilmez et al., 2017). While the optimization problem is the same, the way that the input for the algorithm is obtained differs. In our case, we estimate the combined empirical variogram  $\bar{\Gamma}$  in (26) from samples of the Hüsler–Reiss distribution and derive from this the matrix  $S$  as in Lemma 6.1. In the graph Laplacian learning literature typically the matrix  $S$  is estimated directly from Gaussian data.

We compare our block coordinate descent algorithm described in Algorithm 1 with existing methods for numerical optimization of (30). The first method by Egilmez et al. (2017) is the combinatorial graph Laplacian (CGL) algorithm. For the same problem, Zhao et al. (2019) propose an alternating direction method of multipliers (ADMM) and a majorization-minimization (MM) algorithm, whereas Ying et al. (2021) use an adaptive Laplacian constrained precision matrix estimation (ALPE). For the CGL, ADMM and MM algorithms we use the implementations in the R package `spectralGraphTopology` (Vinicius and Palomar, 2019), and for the ALPE method we use the code from the R package `sparseGraph` (Vinicius et al., 2021). Since the CGL algorithm did not converge in any of our settings, we do not consider it further.

In order to compare the computation times of the different algorithms and the corresponding precision of the numerical solution, we conduct the following study. We first generate a random variogram matrix  $\Gamma$  as the Euclidean distance matrix of  $d$  randomly sampled points from the  $(d-1)$ -dimensional unit sphere. For a given tolerance, we run each algorithm with input given by this matrix  $\Gamma$  (or the corresponding matrix  $S$ ). Since implementation of the tolerances of the algorithms are not directly comparable, we repeat this procedure several times with different variograms and different tolerances each time.

In Figure 1 we show the results for  $d = 50$  by plotting the duality gap in (41) and the corresponding computation times of the different methods. We first observe that the ADMM and the ALPE algorithm do not converge for many simulations. The MM algorithm and our `emtp2` algorithm converge in all cases, but we see that our algorithm is much faster for the same accuracy in terms of

the duality gap. Even for those simulations where ADMM and ALPE converge, our block coordinate descent algorithm usually has a smaller computation time. Figure 2 show the same for dimension  $d = 100$ , where we had to exclude the MM algorithm because of its huge computation times. Again, we observe that our **empt2** algorithm is faster and, more importantly, much more stable than the competing methods.

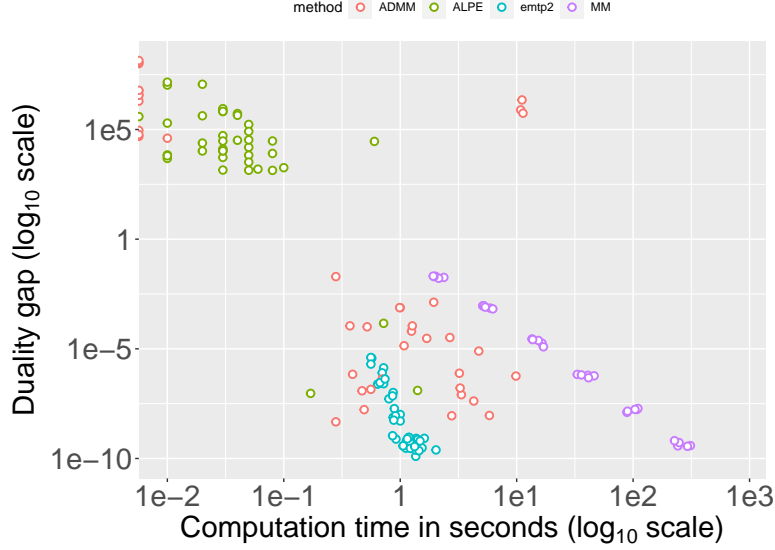


FIGURE 1. Comparison of the algorithms **empt2**, ADMM, MM and ALPE for  $d = 50$  in terms of computation time and duality gap.

Since the **empt2** algorithm is the only one that can be run in higher dimensions, in Table 1 we investigate its computation times for a range of dimensions  $d$ . We observe that even for higher dimension, the algorithm can be applied in a reasonable time. This may be of interest in applications in high-dimensional statistics where regularization is needed.

All computations in this section were made on a laptop with an Intel Core i5 processor with 1.6GHz.

| $d$              | 50   | 100  | 200   | 400    |
|------------------|------|------|-------|--------|
| computation time | 1.00 | 6.95 | 70.55 | 910.76 |

TABLE 1. Average computation times (in seconds) of our **empt2** algorithm from 10 simulations for a tolerance of  $10^{-5}$  and different dimensions  $d$ .

## 8. APPLICATION

**8.1. Data in the domain of attraction.** In this section we illustrate the effectiveness of our method by applying it to the extremes of two data sets, the **carcass** data (Dethlefsen and Højsgaard, 2005) and the **danube** data (Engelke et al., 2020). While in Section 6.1 we assumed to have data points directly from the Hüsler–Reiss distribution  $\mathbf{Y}$ , in practice we usually observe data from a non-extreme random vector  $\tilde{\mathbf{X}}$  to which we apply a preliminary normalization and thresholding step to select the

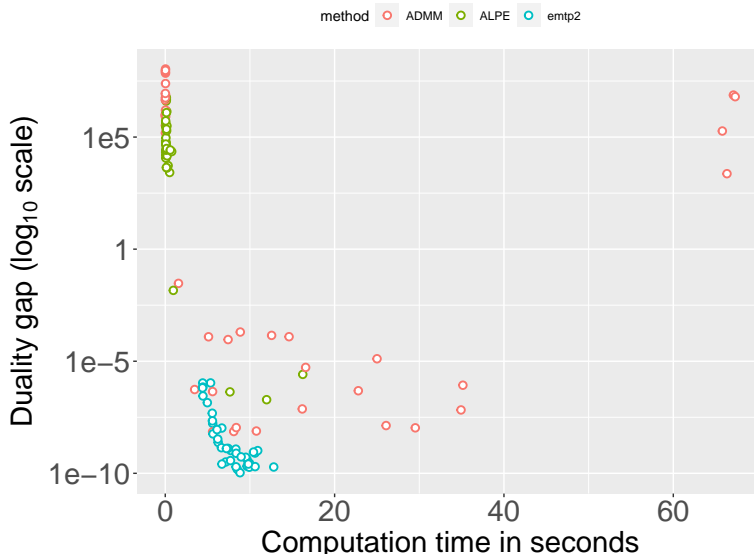


FIGURE 2. Comparison of the algorithms `emtp2`, ADMM and ALPE for  $d = 100$  in terms of computation time and duality gap.

relevant extremes. Following the theory in Section 3.1, we assume that  $\tilde{\mathbf{X}}$  has continuous marginal distribution functions  $F_j$ ,  $j \in [d]$ , and define a normalized random vector  $\mathbf{X}$  with components

$$(42) \quad X_j = 1/\{1 - F_j(\tilde{X}_j)\}, \quad j \in [d],$$

with standard Pareto margins. We assume that it is multivariate regularly varying and in the domain of attraction of  $\mathbf{Y}$  in the sense of (8). For a data matrix  $\tilde{x} \in \mathbb{R}^{n \times d}$  containing  $m$  observations of  $\tilde{\mathbf{X}}$  in the rows, we obtain a data matrix  $x \in \mathbb{R}^{n \times d}$  by applying the transformation (42), with  $F_j$  replaced by the empirical distribution functions  $\hat{F}_j$ , to the columns of the matrix  $\tilde{x}$ . The rows of  $x$ , denoted by  $\mathbf{x}_i$ ,  $i \in [m]$ , are approximate observations of  $\mathbf{X}$ . In a second step, we define the exceedances over some high threshold  $u$  as all observations

$$\mathbf{y}_i = \mathbf{x}_i/u, \quad \text{for all } i \in \mathcal{I} = \{l \in [m] : \|\mathbf{x}_l\|_\infty > u\},$$

where the number of exceedances  $n = |\mathcal{I}|$  depends on the threshold  $u$ . If  $u$  is sufficiently large, by (8) the vectors  $\mathbf{y}_i$ ,  $i \in \mathcal{I}$ , are approximate observations of  $\mathbf{Y}$ . We may now follow the steps in Section 6.1 to compute the combined empirical variogram  $\bar{\Gamma}$  based on these data.

Under some regularity conditions, the approximations described above can be made precise to show that the estimator  $\bar{\Gamma}$  converges to the true  $\Gamma$  as  $m \rightarrow \infty$  and  $n/m \rightarrow 0$  (Engelke and Volgushev, 2020, Theorem 1). Similarly to Proposition 6.6, it then directly follows from the continuity of the EMTP<sub>2</sub> algorithm proved in Proposition 6.5 that the EMTP<sub>2</sub> estimator  $\hat{\Gamma}$  is also consistent for  $\bar{\Gamma}$  based on data in the domain of attraction of  $\mathbf{Y}$ .

**8.2. Carcass data.** The `carcass` data set from the `gRbase` (Dethlefsen and Højsgaard, 2005) package contains measurements of the thickness of different fat and meat layers of  $m = 344$  slaughter pigs. It has been studied in the context of total positivity in the Gaussian case, where Lauritzen et al. (2019) obtain to a sparse graph estimate similar to results obtained from other methods like for example the graphical lasso. They argue that this indicates that the assumption of total positivity should be

reasonable. They restricted the data to the first six variables since the joint distribution including the seventh variable (lean meat) would naturally violate total positivity constraints. We follow this approach and model the extremes of the data  $\tilde{x} \in \mathbb{R}^{m \times d}$  containing  $m = 344$  observations of the first  $d = 6$  variables with an EMTP<sub>2</sub> Hüsler–Reiss model. The purpose of considering this low dimensional data set is mostly to illustrate the impact of the EMTP<sub>2</sub> regularization on the matrices  $\bar{\Gamma}$  and  $\bar{\Theta}$ .

We transform our data as described in Section 8.1 with a threshold  $u$  corresponding to the  $p = 0.9$  quantile of the marginal standard Pareto distribution, resulting in a data matrix  $y \in \mathbb{R}^{n \times d}$  with  $n = 101$  rows containing the exceedances with approximate distribution of  $\mathbf{Y}$ . The combined empirical variogram estimated from these data and the corresponding Hüsler–Reiss precision matrix are

$$\bar{\Gamma} = \begin{pmatrix} 0.00 & 2.50 & 0.56 & 2.22 & 0.97 & 2.51 \\ 2.50 & 0.00 & 2.25 & 0.92 & 2.27 & 0.79 \\ 0.56 & 2.25 & 0.00 & 2.32 & 0.71 & 2.41 \\ 2.22 & 0.92 & 2.32 & 0.00 & 2.44 & 0.52 \\ 0.97 & 2.27 & 0.71 & 2.44 & 0.00 & 2.46 \\ 2.51 & 0.79 & 2.41 & 0.52 & 2.46 & 0.00 \end{pmatrix}, \bar{\Theta} = \begin{pmatrix} 2.11 & 0.26 & -1.54 & -0.64 & -0.40 & 0.21 \\ 0.26 & 1.57 & -0.27 & -0.50 & -0.23 & -0.82 \\ -1.54 & -0.27 & 2.68 & 0.27 & -0.99 & -0.15 \\ -0.64 & -0.50 & 0.27 & 2.39 & 0.14 & -1.64 \\ -0.40 & -0.23 & -0.99 & 0.14 & 1.59 & -0.11 \\ 0.21 & -0.82 & -0.15 & -1.64 & -0.11 & 2.50 \end{pmatrix}.$$

Note that  $\bar{\Theta}$  is almost a Laplacian matrix, indicating intrinsic positivity in the data. We obtain the EMTP<sub>2</sub> Hüsler–Reiss estimate  $(\hat{\Gamma}, \hat{\Theta})$  of the variogram and the precision matrices as the solution of Algorithm 1. They are given by

$$\hat{\Gamma} = \begin{pmatrix} 0.00 & \mathbf{2.27} & 0.56 & 2.22 & 0.97 & \mathbf{2.37} \\ \mathbf{2.27} & 0.00 & 2.25 & 0.92 & 2.27 & 0.79 \\ 0.56 & 2.25 & 0.00 & \mathbf{2.30} & 0.71 & 2.41 \\ 2.22 & 0.92 & \mathbf{2.30} & 0.00 & \mathbf{2.39} & 0.52 \\ 0.97 & 2.27 & 0.71 & \mathbf{2.39} & 0.00 & 2.46 \\ \mathbf{2.37} & 0.79 & 2.41 & 0.52 & 2.46 & 0.00 \end{pmatrix}, \hat{\Theta} = \begin{pmatrix} 2.00 & \mathbf{0.00} & -1.45 & -0.24 & -0.32 & \mathbf{0.00} \\ \mathbf{0.00} & 1.54 & -0.09 & -0.41 & -0.18 & -0.85 \\ -1.45 & -0.09 & 2.60 & \mathbf{0.00} & -1.04 & -0.02 \\ -0.24 & -0.41 & \mathbf{0.00} & 2.23 & \mathbf{0.00} & -1.58 \\ -0.32 & -0.18 & -1.04 & \mathbf{0.00} & 1.57 & -0.03 \\ \mathbf{0.00} & -0.85 & -0.02 & -1.58 & -0.03 & 2.48 \end{pmatrix}.$$

In the matrix  $\hat{\Gamma}$  we marked in bold those entries that differ from the empirical version  $\bar{\Gamma}$ . In the precision matrix  $\hat{\Theta}$  we marked in bold those entries that have been set to zero by the EMTP<sub>2</sub> constraint. We observe that these are in correspondence, and that in comparison with  $\bar{\Gamma}$  only few entries in  $\hat{\Gamma}$  have changed. This is a consequence of the fact that the EMTP<sub>2</sub> solution  $(\hat{\Gamma}, \hat{\Theta})$  must satisfy the KKT conditions in Theorem 6.3. In particular, Condition (iii) of this theorem imposes zeros in  $\hat{\Theta}$  exactly where  $\hat{\Gamma}$  differs from  $\bar{\Gamma}$ . By (21), this implies that the Hüsler–Reiss distribution is an extremal graphical model as defined in Engelke and Hitz (2020), demonstrating how EMTP<sub>2</sub> enforces sparsity.

**8.3. Danube data.** For an application that is more relevant in terms of risk assessment, we consider river discharge data from the upper Danube basin, which were originally used in Asadi et al. (2015). The data set consists of daily measurements collected at  $d = 31$  gauging stations over 50 years of from 1960 to 2009 by the Bavarian Environmental Agency (<http://www.gkd.bayern.de>). After declustering and selecting only the summer months, Asadi et al. (2015) obtain  $m = 428$  observations that are assumed independent. The **danube** data are available in the R package **graphicalExtremes** and have been studied in a number of papers with focus on the modeling of extremal dependence (Asadi et al., 2015; Engelke and Hitz, 2020) and detecting the extremal causal structure (Tran et al., 2021; Mhalla et al., 2020; Gnecco et al., 2021). For more details on the data and the preprocessing we refer to Asadi et al. (2015). We normalize the data as described in Section 8.1 and, following Engelke and Hitz (2020), we chose the  $p = 0.9$  quantile of the marginal Pareto distribution as threshold  $u$ , which results in a dataset of  $n = 116$  observations.

In order to compare our method to existing approaches, we fit several different Hüsler–Reiss models to the data, some with graphical structure, and some without. The first naive approach is to use the

combined extremal variogram  $\bar{\Gamma}$ , which corresponds to a trivial, fully connected graph. As a simple extremal graphical model based on domain knowledge we consider a Hüsler–Reiss distribution on the undirected tree given by the physical flow connection of the river network. As an alternative tree model, we fit the minimum spanning tree based on  $\bar{\Gamma}$ , which is a consistent estimator of the extremal graph structure if the true graph is a tree (Engelke and Volgushev, 2020). As discussed in Engelke and Hitz (2020), a tree might be too restrictive, and following their methodology, we fit a sequence of extremal block graph models and choose the best one according to AIC. Asadi et al. (2015) propose a model from spatial extreme value statistics that heavily relies on domain knowledge of this data set, such as catchment sizes and distances between stations. We fit their model in our framework and remark that it has six parameters but corresponds to a fully connected graph. Finally, we compute our Hüsler–Reiss estimator under the EMTP<sub>2</sub> constraint. This results in a sparse estimator  $\bar{\Theta}$  and the corresponding extremal graph is shown in Figure 3. For the sake of fair comparison, we do not use censoring in any of the approaches here (cf., Smith et al., 1997). For the EMTP<sub>2</sub> estimator, censoring could be achieved by using a censored estimator of  $\Gamma$  in the input of Algorithm 1.

The results of the model fits can be found in Table 2. Among the graphical models, both in terms of AIC and BIC, we observe that our EMTP<sub>2</sub> performs best. This is remarkable since our method does not have any tuning parameters and the assumption of EMTP<sub>2</sub> might seem restrictive. The good performance suggests that the extremes of this data exhibit strong positive dependence, which underlines the theoretical findings of this paper. The spatial model of Asadi et al. (2015) performs similarly to our EMTP<sub>2</sub> estimator in terms of AIC, and in terms of BIC, which penalizes the number of model parameters more strongly, the spatial model is first. We note that this comparison is flawed since, as opposed to the spatial model, our estimator is completely data-driven and does not use any domain knowledge. It can therefore easily be applied to general multivariate data where no information of the gauging stations is available, as for instance for the `carcass` data.

For our EMTP<sub>2</sub> approach, the graph is a side product and there is no guarantee of correct graph recovery. Interestingly, the EMTP<sub>2</sub> graph in Figure 3 resembles the structures that are obtained from the minimum spanning tree and the block graph. The latter are methods designed to detect and model conditional independences. For instance, the EMTP<sub>2</sub> graph contains all physical flow connections with the exception of the edges (25, 4) and (20, 7); see also the geographical map of the upper Danube basin in Asadi et al. (2015, Figure 1). Most of the additional connections resemble geographical proximity or similarity, which may correspond to positive extremal dependence between such nodes.

|                             | twice neg logLH | nb par | AIC     | BIC     |
|-----------------------------|-----------------|--------|---------|---------|
| empirical variogram         | 270.58          | 465    | 1200.58 | 2484.99 |
| flow graph                  | 1465.22         | 30     | 1525.22 | 1608.08 |
| MST                         | 1390.04         | 30     | 1450.04 | 1532.90 |
| best block graph MST        | 1263.55         | 42     | 1347.55 | 1463.57 |
| Asadi et al.                | 1107.78         | 6      | 1119.78 | 1136.35 |
| EMTP <sub>2</sub> estimator | 1034.42         | 67     | 1168.42 | 1353.49 |

TABLE 2. Results for the different models fitted to the Danube river data set; columns show twice the negative log-likelihood, the number of model parameters and the AIC and BIC values, respectively.

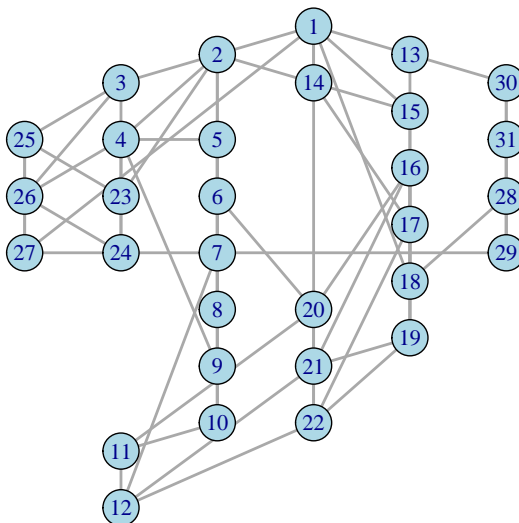


FIGURE 3. Extremal graphical structure of the fitted  $\text{EMTP}_2$  Hüsler–Reiss distribution.

**Acknowledgements.** Sebastian Engelke and Frank Röttger were supported by the Swiss National Science Foundation (Grant 186858). Piotr Zwiernik was supported by the Spanish Ministry of Economy and Competitiveness (Grant PGC2018-101643-B-I00) and the Ramón y Cajal fellowship (RYC-2017-22544).

#### REFERENCES

- Agrawal, R., U. Roy, and C. Uhler (2020). Covariance matrix estimation under total positivity for portfolio selection. *Journal of Financial Econometrics*.
- Asadi, P., A. C. Davison, and S. Engelke (2015). Extremes on river networks. *The Annals of Applied Statistics* 9(4), 2023 – 2050.
- Banerjee, O., L. El Ghaoui, and A. d’Aspremont (2008). Model selection through sparse maximum likelihood estimation for multivariate Gaussian or binary data. *The Journal of Machine Learning Research* 9, 485–516.
- Berge, C. (1997). *Topological spaces*. Dover Publications, Inc., Mineola, NY. Including a treatment of multi-valued functions, vector spaces and convexity, Translated from the French original by E. M. Patterson, Reprint of the 1963 translation.
- Bertsekas, D. P. (2009). *Convex optimization theory*. Athena Scientific, Nashua, NH.
- Boyd, S. and L. Vandenberghe (2004). *Convex optimization*. Cambridge University Press, Cambridge.
- Coles, S. G. and J. A. Tawn (1991). Modelling extreme multivariate events. *Journal of the Royal Statistical Society. Series B (Methodological)* 53(2), 377–392.

- de Haan, L. and A. Ferreira (2006). *Extreme Value Theory*. New York: Springer.
- Dellacherie, C., S. Martinez, and J. San Martin (2014). *Inverse  $M$ -matrices and ultrametric matrices*, Volume 2118. Springer.
- Dethlefsen, C. and S. Højsgaard (2005). A common platform for graphical models in R: the gRbase package. *Journal of Statistical Software* 14(17), 1–12.
- Devriendt, K. (2020). Effective resistance is more than distance: Laplacians, simplices and the Schur complement.
- Dombry, C., S. Engelke, and M. Oesting (2016). Exact simulation of max-stable processes. *Biometrika* 103, 303–317.
- Dombry, C. and F. Eyi-Minko (2013). Regular conditional distributions of continuous max-infinitely divisible random fields. *Electronic Journal of Probability* 18, 1 – 21.
- Drees, H. and A. Sabourin (2021). Principal component analysis for multivariate extremes. *Electronic Journal of Statistics* 15(1), 908 – 943.
- Duval, A., C. Klivans, and J. Martin (2009). Simplicial matrix-tree theorems. *Transactions of the American Mathematical Society* 361(11), 6073–6114.
- Egilmez, H. E., E. Pavez, and A. Ortega (2017). Graph learning from data under Laplacian and structural constraints. *IEEE Journal of Selected Topics in Signal Processing* 11(6), 825–841.
- Embrechts, P., C. Klüppelberg, and T. Mikosch (1997). *Modelling Extremal Events: for Insurance and Finance*. London: Springer.
- Engelke, S. and A. S. Hitz (2020). Graphical models for extremes (with discussion). *Journal of the Royal Statistical Society: Series B (Statistical Methodology)* 82(4), 871–932.
- Engelke, S., S. A. Hitz, and N. Gnecco (2020). *graphicalExtremes: Statistical Methodology for Graphical Extreme Value Models*. Available from <https://github.com/sebastian-engelke/graphicalExtremes>.
- Engelke, S. and J. Ivanovs (2021). Sparse structures for multivariate extremes. *Annual Review of Statistics and Its Application* 8, 241–270.
- Engelke, S., A. Malinowski, Z. Kabluchko, and M. Schlather (2015). Estimation of Hüsler–Reiss distributions and Brown–Resnick processes. *Journal of the Royal Statistical Society: Series B (Statistical Methodology)* 77, 239–265.
- Engelke, S. and S. Volgushev (2020). Structure learning for extremal tree models. *arXiv preprint arXiv:2012.06179*.
- Esary, J. D., F. Proschan, and D. W. Walkup (1967). Association of random variables, with applications. *The Annals of Mathematical Statistics* 38(5), 1466–1474.
- Fallat, S., S. Lauritzen, K. Sadeghi, C. Uhler, N. Wermuth, and P. Zwiernik (2017). Total positivity in Markov structures. *The Annals of Statistics* 45(3), 1152–1184.
- Farris, J. S., A. G. Kluge, and M. J. Eckardt (1970). A numerical approach to phylogenetic systematics. *Systematic Zoology* 19(2), 172–189.
- Felsenstein, J. (1973). Maximum-likelihood estimation of evolutionary trees from continuous characters. *American journal of human genetics* 25(5), 471.
- Fiedler, M. (1998). Some characterizations of symmetric inverse  $M$ -matrices. In *Proceedings of the Sixth Conference of the International Linear Algebra Society (Chemnitz, 1996)*, Volume 275/276, pp. 179–187.
- Fortuin, C. M., P. W. Kasteleyn, and J. Ginibre (1971). Correlation inequalities on some partially ordered sets. *Communications in Mathematical Physics* 22, 89–103.
- Gissibl, N. and C. Klüppelberg (2018). Max-linear models on directed acyclic graphs. *Bernoulli* 24, 2693–2720.
- Gnecco, N., N. Meinshausen, J. Peters, and S. Engelke (2021). Causal discovery in heavy-tailed models. *The Annals of Statistics* 49(3), 1755–1778.



- Gower, J. C. (1985). Properties of Euclidean and non-Euclidean distance matrices. *Linear Algebra and its Applications* 67, 81–97.
- Hentschel, M. (2021). *Statistical Inference for Hüsler–Reiss Graphical Models*. Master thesis, Universität Mannheim.
- Højsgaard, S., D. Edwards, and S. Lauritzen (2012). *Graphical models with R*. Springer Science & Business Media.
- Holbrook, A. (2018). Differentiating the pseudo determinant. *Linear Algebra and its Applications* 548, 293–304.
- Hüsler, J. and R.-D. Reiss (1989). Maxima of normal random vectors: between independence and complete dependence. *Statistics & Probability Letters* 7(4), 283–286.
- Janßen, A. and P. Wan (2020).  $k$ -means clustering of extremes. *Electronic Journal of Statistics* 14(1), 1211 – 1233.
- Karlin, S. and Y. Rinott (1980). Classes of orderings of measures and related correlation inequalities. I. Multivariate totally positive distributions. *Journal of Multivariate Analysis* 10(4), 467–498.
- Klein, D. J. and M. Randić (1993). Resistance distance. *Journal of mathematical chemistry* 12(1), 81–95.
- Lauritzen, S. (1996). *Graphical Models*. Oxford Statistical Science Series. Clarendon Press.
- Lauritzen, S. and K. Sadeghi (2018). Unifying Markov properties for graphical models. *The Annals of Statistics* 46(5), 2251 – 2278.
- Lauritzen, S., C. Uhler, and P. Zwiernik (2019, 08). Maximum likelihood estimation in Gaussian models under total positivity. *Annals of Statistics* 47(4), 1835–1863.
- Lauritzen, S., C. Uhler, and P. Zwiernik (2021). Total positivity in exponential families with application to binary variables. *The Annals of Statistics* 49(3), 1436 – 1459.
- Lauritzen, S. and P. Zwiernik (2020a). *GOLAZO: Flexible regularised likelihood estimation using the GOLAZO approach*. Available from <https://github.com/pzwiernik/golazo>.
- Lauritzen, S. and P. Zwiernik (2020b). Locally associated graphical models and mixed convex exponential families.
- Layer, M. and J. A. Rhodes (2017). Phylogenetic trees and Euclidean embeddings. *Journal of mathematical biology* 74(1-2), 99–111.
- Liu, Y. and T. J. Kozubowski (2015). A folded Laplace distribution. *Journal of Statistical Distributions and Applications* 2(1), 1–17.
- Mhalla, L., V. Chavez-Demoulin, and D. J. Dupuis (2020). Causal mechanism of extreme river discharges in the upper Danube basin network. *Journal of the Royal Statistical Society: Series C (Applied Statistics)* 69(4), 741–764.
- Micchelli, C. A. (1986). Interpolation of scattered data: distance matrices and conditionally positive definite functions. *Constructive approximation* 2(1), 11–22.
- Murota, K. (2009). Recent developments in discrete convex analysis. In *Research trends in combinatorial optimization*, pp. 219–260. Springer.
- Newman, C. M. (1983). A general central limit theorem for FKG systems. *Communications in mathematical physics* 91(1), 75–80.
- Newman, C. M. (1984). Asymptotic independence and limit theorems for positively and negatively dependent random variables. *Lecture Notes-Monograph Series* 5, 127–140.
- Pearl, J. (2009). *Causality* (2 ed.). Cambridge University Press.
- Pitt, L. D. (1982, 05). Positively correlated normal variables are associated. *Annals of Probability* 10(2), 496–499.
- Ravikumar, P., M. J. Wainwright, G. Raskutti, and B. Yu (2011). High-dimensional covariance estimation by minimizing  $\ell_1$ -penalized log-determinant divergence. *Electronic Journal of Statistics* 5, 935–980.

- Resnick, S. I. (2008). *Extreme Values, Regular Variation and Point Processes*. New York: Springer.
- Robeva, E., B. Sturmfels, N. Tran, and C. Uhler (2021). Maximum likelihood estimation for totally positive log-concave densities. *Scandinavian Journal of Statistics* 48(3), 817–844.
- Rockafellar, R. T. (2015). *Convex analysis*. Princeton university press.
- Rootzén, H. and N. Tajvidi (2006). Multivariate generalized Pareto distributions. *Bernoulli. Official Journal of the Bernoulli Society for Mathematical Statistics and Probability* 12, 917–930.
- Rossell, D. and P. Zwiernik (2021). Dependence in elliptical partial correlation graphs. *Electronic Journal of Statistics* 15(2), 4236–4263.
- Schoenberg, I. J. (1935). Remarks to Maurice Fréchet’s article “Sur la définition axiomatique d’une classe d’espace distanciés vectoriellement applicable sur l’espace de Hilbert” [MR1503246]. *Annals of Mathematics. Second Series* 36(3), 724–732.
- Segers, J. (2020). One- versus multi-component regular variation and extremes of Markov trees. *Advances in Applied Probability* 52(3), 855–878.
- Semple, C., M. Steel, et al. (2003). *Phylogenetics*, Volume 24. Oxford University Press on Demand.
- Slawski, M. and M. Hein (2015). Estimation of positive definite M-matrices and structure learning for attractive Gaussian Markov random fields. *Linear Algebra and its Applications* 473, 145 – 179. Special issue on Statistics.
- Smith, R., J. Tawn, and S. Coles (1997). Markov chain models for threshold exceedances. *Biometrika* 84, 249–268.
- Spirtes, P., C. N. Glymour, R. Scheines, and D. Heckerman (2000). *Causation, prediction, and search*. MIT press.
- Stellato, B., G. Banjac, P. Goulart, A. Bemporad, and S. Boyd (2020). OSQP: an operator splitting solver for quadratic programs. *Mathematical Programming Computation* 12(4), 637–672.
- Sturmfels, B., C. Uhler, and P. Zwiernik (2020). Brownian motion tree models are toric. *Kybernetika* 56, 1154–1175.
- Tawn, J. A. (1990). Modelling multivariate extreme value distributions. *Biometrika* 77, 245–253.
- Tran, N. M., J. Buck, and C. Klüppelberg (2021). Estimating a latent tree for extremes.
- Vinicius, Z. and D. Palomar (2019). *spectralGraphTopology: Learning Graphs from Data via Spectral Constraints*. Available from <https://cran.r-project.org/package=spectralGraphTopology>.
- Vinicius, Z., J. Ying, and D. Palomar (2021). *sparseGraph: Estimating Graphs with Nonconvex, Sparse Promoting Regularizations*. Available from <https://github.com/mirca/sparseGraph/>.
- Wang, Y., U. Roy, and C. Uhler (2020). Learning high-dimensional Gaussian graphical models under total positivity without adjustment of tuning parameters. In S. Chiappa and R. Calandra (Eds.), *Proceedings of the Twenty Third International Conference on Artificial Intelligence and Statistics*, Volume 108 of *Proceedings of Machine Learning Research*, pp. 2698–2708. PMLR.
- Ying, J., J. M. Cardoso, and D. Palomar (2021). Minimax estimation of Laplacian constrained precision matrices. In *International Conference on Artificial Intelligence and Statistics*, pp. 3736–3744. PMLR.
- Zhao, L., Y. Wang, S. Kumar, and D. Palomar (2019). Optimization algorithms for graph Laplacian estimation via ADMM and MM. *IEEE Transactions on Signal Processing* 67(16), 4231–4244.

#### APPENDIX A. THE ALGEBRA OF VARIOGRAM MATRICES

**A.1. Algebraic structure.** Let  $\mathbb{S}^d$  be the space of real symmetric  $d \times d$  matrices and  $\mathbb{S}_0^d$  its subspace with zeros on the diagonal. We equip  $\mathbb{S}^d$  with the standard trace inner product  $\langle A, B \rangle = \text{tr}(AB) = \sum_{i,j} A_{ij}B_{ij}$  and  $\mathbb{S}_0^d$  with  $\langle\langle A, B \rangle\rangle = \sum_{i < j} A_{ij}B_{ij}$ . For  $\mathbf{b} \in \mathbb{R}^d$  satisfying  $\mathbf{b}^T \mathbf{1} = 1$  we define:

- (i) linear subspace of  $\mathbb{S}^d$ :  $\mathbb{U}_{\mathbf{b}} = \{A \in \mathbb{S}^d : A\mathbf{b} = \mathbf{0}\}$ ,
- (ii) projection on  $\mathbb{R}^d/\mathbf{1}$ :  $\mathbf{P}_{\mathbf{b}} = I_d - \mathbf{1}\mathbf{b}^T$ ,

(iii) linear map:  $\sigma_{\mathbf{b}} : \mathbb{S}_0^d \rightarrow \mathbb{U}_{\mathbf{b}}, A \mapsto \mathbf{P}_{\mathbf{b}}(-\frac{A}{2})\mathbf{P}_{\mathbf{b}}^T$ .

It is useful to note that for any  $\mathbf{a}, \mathbf{b}$  such that  $\mathbf{a}^T \mathbf{1} = \mathbf{b}^T \mathbf{1} = 1$

$$(43) \quad \mathbf{P}_{\mathbf{a}} \mathbf{P}_{\mathbf{b}} = \mathbf{P}_{\mathbf{a}}.$$

The relevant cases for us are when  $\mathbf{b} = \frac{1}{d}\mathbf{1}$  and when  $\mathbf{b} = \mathbf{e}_k$  is a canonical unit vector. If  $\mathbf{b} = \frac{1}{d}\mathbf{1}$ , we omit the subscript writing  $\mathbb{U}$  and  $\mathbf{P}$ . In the special case when  $\mathbf{b} = \mathbf{e}_k$ , we write  $\mathbf{P}_k$  and  $\mathbb{U}_k$ . Note that  $\mathbf{P}$  is symmetric and it represents the *orthogonal* projection matrix on  $\mathbb{R}^d/\mathbf{1}$ . Also  $\mathbf{P}_k$  has rows  $\mathbf{e}_i - \mathbf{e}_k$  and, in particular, the  $k$ th row is zero. We denote by  $\bar{\mathbf{P}}_k \in \mathbb{R}^{(d-1) \times d}$  the matrix obtained from  $\mathbf{P}_k$  by removing the  $k$ th row.

Let  $\mathbb{S}_0^d[\Gamma], \mathbb{S}_0^d[Q]$  be two copies of  $\mathbb{S}_0^d$  with coordinates denoted by  $\Gamma_{ij}$  and  $Q_{ij}$  respectively. Similarly, we let  $\mathbb{U}_{\mathbf{b}}[\Sigma], \mathbb{U}_{\mathbf{b}}[\Theta]$  be two copies of  $\mathbb{U}_{\mathbf{b}}$ . Consider the following sequence of transformations

$$\mathbb{S}_0^d[\Gamma] \xrightarrow{\sigma_{\mathbf{b}}} \mathbb{U}_{\mathbf{b}}[\Sigma] \xrightarrow{\text{ginv}} \mathbb{U}_{\mathbf{b}}[\Theta] \xrightarrow{\sigma_{\mathbf{b}}^*} \mathbb{S}_0^d[Q],$$

where ginv stands for the generalized inverse  $\Sigma \mapsto \Sigma^+$ ,  $\sigma_{\mathbf{b}}$  is a linear map defined by  $\sigma_{\mathbf{b}}(\Gamma) = \mathbf{P}_{\mathbf{b}}(-\frac{1}{2}\Gamma)\mathbf{P}_{\mathbf{b}}^T$ , and  $\sigma_{\mathbf{b}}^*$  denotes the adjoint of the linear map  $\sigma_{\mathbf{b}}$ , that is, the unique transformation that satisfies

$$(44) \quad \langle \sigma_{\mathbf{b}}(\Gamma), \Theta \rangle = \langle \Gamma, \sigma_{\mathbf{b}}^*(\Theta) \rangle \quad \text{for all } \Gamma \in \mathbb{S}_0^d, \Theta \in \mathbb{U}_{\mathbf{b}}.$$

**Remark A.1.** We note that:

- (1) The map  $\sigma_{\mathbf{b}}$  is invertible with the inverse  $\gamma_{\mathbf{b}} : \mathbb{U}_{\mathbf{b}} \rightarrow \mathbb{S}_0^d$  given by

$$\gamma_{\mathbf{b}}(\Sigma) = (\Sigma_{ii} + \Sigma_{jj} - 2\Sigma_{ij})_{i < j}.$$

- (2) Standard linear algebra gives that the adjoint of the inverse  $\gamma_{\mathbf{b}}$  is equal to the inverse of the adjoint  $\sigma_{\mathbf{b}}^*$ .
- (3) The generalized inverse is a well-defined automorphism on  $\mathbb{U}_{\mathbf{b}}$ .
- (4) The inner products are preserved in the sense that for every  $\Gamma, Q \in \mathbb{S}_0^d$  with  $\Sigma = \sigma_{\mathbf{b}}(\Gamma)$  and  $\Theta = \gamma_{\mathbf{b}}^*(Q)$  we have that

$$\langle \Sigma, \Theta \rangle = \langle \sigma_{\mathbf{b}}(\Gamma), \gamma_{\mathbf{b}}^*(Q) \rangle = \langle \gamma_{\mathbf{b}}(\sigma_{\mathbf{b}}(\Gamma)), Q \rangle = \langle \Gamma, Q \rangle.$$

The adjoint map can be easily computed and its form is particularly simple in the special case when  $\mathbf{b} = \frac{1}{d}\mathbf{1}$  and when  $\mathbf{b} = \mathbf{e}_k$ . To avoid confusion we introduce different notation for the coordinates of  $\mathbb{S}_0^d$  and  $\mathbb{U}_{\mathbf{b}}$  depending on a particular  $\mathbf{b}$ . We use

- (i)  $\Sigma, \Theta$  to denote coordinates in  $\mathbb{U}$ ,
- (ii)  $\tilde{\Sigma}^{(k)}, \tilde{\Theta}^{(k)}$  to denote coordinates in  $\mathbb{U}_k$ , and
- (iii)  $\Sigma^{(k)}, \Theta^{(k)}$  to denote matrices in  $\mathbb{S}^{d-1}$  obtained from  $\tilde{\Sigma}^{(k)}, \tilde{\Theta}^{(k)}$  by removing the  $k$ th row/column.

**Lemma A.2.** *The adjoint map  $\sigma^* : \mathbb{U}[\Theta] \rightarrow \mathbb{S}_0^d[Q]$  is given by  $Q_{ij} = -\Theta_{ij}$  for all  $1 \leq i < j \leq d$ . The adjoint map  $\sigma_k^* : \mathbb{U}_k[\tilde{\Theta}^{(k)}] \rightarrow \mathbb{S}_0^d[Q]$  is given by  $Q_{ij} = -\Theta_{ij}^{(k)}$  for all  $i, j \neq k$  and  $Q_{ik} = \sum_{j \neq k} \Theta_{ij}^{(k)}$ .*

*Proof.* The adjoint maps are defined by (44). We will check this condition on the basis of  $\mathbb{S}_0^d$  given by elements of the form  $B = E_{ij} + E_{ji}$ , where  $E_{ij}$  denotes the elementary matrix with the  $ij$ th entry equal to one and zero otherwise. Let first  $\mathbf{b} = \frac{1}{d}\mathbf{1}$ . The right-hand side of (44) becomes  $(\sigma^*(\Theta))_{ij}$ . The left hand side is

$$\langle \mathbf{P}(-\frac{B}{2})\mathbf{P}, \Theta \rangle = -\frac{1}{2}\text{tr}(B\mathbf{P}\Theta\mathbf{P}) = -\frac{1}{2}\text{tr}(B\Theta) = -\Theta_{ij},$$

where we used the fact that  $\mathbf{P}\Theta\mathbf{P} = \Theta$  for all  $\Theta \in \mathbb{U}$ . The second part of the result follows similar calculations and the fact that  $(\mathbf{P}_k^T \tilde{\Theta}^{(k)} \mathbf{P}_k)_{ij} = \Theta_{ij}^{(k)}$  if  $i, j \neq k$  and  $(\mathbf{P}_k^T \tilde{\Theta}^{(k)} \mathbf{P}_k)_{ik} = -\sum_{j \neq k} \Theta_{ij}^{(k)}$ .  $\square$

In our paper we start with the variogram matrix  $\Gamma \in \mathbb{S}_0^d$ . The matrix  $\Sigma^{(k)}$  defined in (11) is a  $(d-1) \times (d-1)$  matrix obtained from  $\sigma_k(\Gamma) \in \mathbb{U}_k$  by removing the  $k$ th row/column. The inverse of  $\sigma_k$  expresses  $\Gamma$  in terms of  $\Sigma^{(k)}$  as in (12). The matrix  $\Theta = \Sigma^+ = (\mathbf{P}(-\frac{1}{2}\Gamma)\mathbf{P})^+$  is exactly the same matrix that appears in Proposition 3.3. To easily translate between various equivalent representations of the variogram matrix  $\Gamma$  we define  $f_k : \mathbb{U} \rightarrow \mathbb{U}_k$  by  $\Sigma \mapsto \mathbf{P}_k \Sigma \mathbf{P}_k^T$ . The following results provides the complete picture of the situation.

**Proposition A.3.** *The adjoint  $f_k^* : \mathbb{U}_k \rightarrow \mathbb{U}$  of  $f_k$  is defined by  $\Theta \mapsto \mathbf{P}_k^T \Theta \mathbf{P}_k$ . Moreover, the following diagram commutes<sup>1</sup>*

$$\begin{array}{ccccc}
 \mathbb{S}^{d-1}[\Sigma^{(k)}] & \xrightarrow{\text{inv}} & \mathbb{S}^{d-1}[\Theta^{(k)}] & & \\
 \uparrow \pi_k & & \downarrow \pi_k^* & & \\
 \mathbb{S}_0^d[\Gamma] & \xrightarrow{\sigma_k} & \mathbb{U}_k[\tilde{\Sigma}^{(k)}] & \xrightarrow{\text{ginv}} & \mathbb{U}_k[\tilde{\Theta}^{(k)}] & \xrightarrow{\sigma_k^*} & \mathbb{S}_0^d[Q] \\
 \searrow \sigma & & \uparrow f_k & & \downarrow f_k^* & & \nearrow \sigma^* \\
 & & \mathbb{U}[\Sigma] & \xrightarrow{\text{ginv}} & \mathbb{U}[\Theta] & & 
 \end{array}$$

where  $\pi_k$  drops the  $k$ th row/column of  $\tilde{\Sigma}^{(k)}$  and its adjoint  $\pi_k^*$  embeds  $\Theta^{(k)}$  in  $\mathbb{U}_k$  by adding the zero row/column. All the maps apart from the inversion on the top are well defined everywhere. For the inversion we restrict the map to an open subset where  $\Sigma^{(k)}$  is invertible.

*Proof.* To verify the formula for the adjoint  $f_k^*$  we note that, by definition, it must satisfy

$$\langle f_k(\Sigma), \tilde{\Theta}^{(k)} \rangle = \langle \Sigma, f_k^*(\tilde{\Theta}^{(k)}) \rangle \quad \text{for all } \Sigma \in \mathbb{U}, \tilde{\Theta}^{(k)} \in \mathbb{U}_k,$$

and the formula follows by basic properties of the matrix trace and the fact that  $\mathbf{P}_b^T \tilde{\Theta}^{(k)} \mathbf{P}_b \in \mathbb{U}$ .

To verify that the diagram commutes, it is enough to check that that it commutes along two side triangles, that is, that  $\sigma_k = f_k \sigma$  and  $\sigma_k^* = \sigma^* f_k^*$  and along two central rectangles. The bottom rectangle follows by the above calculations. The upper rectangle follows by how pseudoinverse works on the space  $\mathbb{U}_k$ . To see that  $\sigma_k = f_k \sigma$  note that, by (43),

$$f_k(\sigma(\Gamma)) = \mathbf{P}_k \mathbf{P}(-\frac{\Gamma}{2}) \mathbf{P} \mathbf{P}_k^T = \mathbf{P}_k(-\frac{\Gamma}{2}) \mathbf{P}_k^T = \sigma_k(\Gamma).$$

To check that  $\sigma_k^* = \sigma^* f_k^*$  we use basic properties of the adjoint.  $\square$

Proposition A.3 gives us another way to verify formula (13).

**Lemma A.4.** *Fix  $k \in \{1, \dots, d\}$  then the form of the mapping  $f_k^*$  implies that*

$$\Theta_{ij} = \begin{cases} \Theta_{ij}^{(k)} & \text{if } i, j \neq k, \\ -\sum_{l \neq k} \Theta_{il}^{(k)} & \text{if } i \neq k, j = k, \\ \sum_{i, j \neq k} \Theta_{ij}^{(k)} & \text{if } i = j = k. \end{cases}$$

By Lemma A.2,  $\Theta \in \mathbb{U}$  is a weighted Laplacian matrix with potentially negative weights  $Q_{ij}$  for  $i \neq j$ . The Weighted Matrix-Tree Theorem in Lemma 4.4 will be useful for the next result.

**Proposition A.5.** *The mapping  $\mathbb{S}_0^d[\Gamma] \rightarrow \mathbb{S}_0^d[Q]$  given by  $\Gamma \mapsto \sigma_k^*((\sigma_k(\Gamma))^+)$  is compactly written as*

$$Q = \nabla \log \text{Det}(\sigma_k(\Gamma)).$$

Similarly,

$$\Gamma = \nabla \log \text{Det}(\gamma_k^*(Q)).$$

<sup>1</sup>By this we mean that composing maps along any two directed paths with the same beginning and end results in the same function.

*Proof.* Let  $\bar{\Gamma}$  be a given point in  $\mathbb{S}_0^d[\Gamma]$  and let  $\tilde{S}^{(k)} = \sigma_k(\bar{\Gamma}) \in \mathbb{U}_k$ . Similarly, let  $Q^S = \sigma_k^*((\sigma_k(\bar{\Gamma}))^+)$ . By [Holbrook \(2018\)](#),

$$\nabla_{\Sigma}(\log \text{Det}(\Sigma) - \langle \Sigma, (\tilde{S}^{(k)})^+ \rangle) \Big|_{\Sigma=\tilde{S}^{(k)}} = 0.$$

Using the fact that  $\sigma_k : \mathbb{S}_0^d \rightarrow \mathbb{U}_k$  is an invertible linear mapping, we get that equivalently,

$$\nabla_{\Gamma}(\log \text{Det}(\sigma_k(\Gamma)) - \langle \sigma_k(\Gamma), (\tilde{S}^{(k)})^+ \rangle) \Big|_{\Gamma=\bar{\Gamma}} = 0.$$

Since  $\langle \sigma(\Gamma), (\tilde{S}^{(k)})^+ \rangle = \langle \Gamma, \sigma^*((\tilde{S}^{(k)})^+) \rangle = \langle \Gamma, Q^S \rangle$  we obtain the desired formula.  $\square$

**A.2. Strictly conditionally negative matrices.** The variogram matrices are not only assumed to lie in  $\mathbb{S}_0^d$  but they are assumed to be strictly conditionally negative definite. We study this additional constraint a bit more in this section. Using the notation from Section 3.2,  $\Gamma \in \mathcal{C}^d \subset \mathbb{S}_0^d$ . In this section we briefly list relevant results that follow from assuming this extra structure.

**Remark A.6.** If  $\Gamma$  is a conditionally negative definite matrix, then, by the theorem of Schoenberg ([Gower, 1985](#); [Schoenberg, 1935](#)), equivalently, there exist vectors  $\mathbf{y}_1, \dots, \mathbf{y}_d$  in some Euclidean space  $\mathbb{R}^p$  such that  $\Gamma_{ij} = \|\mathbf{y}_i - \mathbf{y}_j\|^2$ . We also call such  $\Gamma$  a Euclidean distance matrix.

**Lemma A.7.** *If  $\Gamma \in \mathcal{C}^d$  then  $\Gamma_{ij} > 0$  for all  $i \neq j$ .*

*Proof.* Take  $\mathbf{x} = \mathbf{e}_i - \mathbf{e}_j$ . By definition  $\mathbf{x}^T \Gamma \mathbf{x} = -2\Gamma_{ij}$  must be strictly negative.  $\square$

**Lemma A.8.** *The cone  $\sigma_b(\mathcal{C}^d)$  is precisely the set of all positive semi-definite matrices in  $\mathbb{U}_b$  of the rank  $d-1$ . The mapping  $\pi_k : \mathbb{U}_k \rightarrow \mathbb{S}^{d-1}$  maps  $\sigma_k(\mathcal{C}^d)$  to the positive definite cone  $\mathbb{S}_+^{d-1}$ .*

*Proof.* Let  $\Gamma \in \mathcal{C}^d$ . Since  $\sigma_b(\Gamma)$  is symmetric it has real eigenvalues and the eigenvectors are mutually orthogonal. It is clear that  $\mathbf{b}^T \sigma_b(\Gamma) \mathbf{b} = 0$  so  $\mathbf{b}$  is an eigenvector with eigenvalue 0. We will show that all the other eigenvalues must be strictly positive. If  $\mathbf{b} = \pm \frac{1}{d} \mathbf{1}$  then  $\mathbf{x} \perp \mathbf{b}$  and  $\mathbf{x} \neq \mathbf{0}$  implies that

$$\mathbf{x}^T \sigma(\Gamma) \mathbf{x} = \mathbf{x}^T (-\frac{1}{2} \Gamma) \mathbf{x} > 0$$

by the fact that  $\Gamma$  is strictly conditionally negative definite. This implies that all the remaining eigenvalues of  $\sigma(\Gamma)$  must be strictly positive. Suppose now that  $\mathbf{b} \neq \pm \frac{1}{d} \mathbf{1}$ . By Proposition A.3,  $\sigma_b(\Gamma) = \mathbf{P}_b \sigma(\Gamma) \mathbf{P}_b^T$ . Since  $\mathbf{P}_b^T \mathbf{x} = \mathbf{x} - (\mathbf{1}^T \mathbf{x}) \mathbf{b}$ ,  $\mathbf{P}_b^T \mathbf{x} \perp \mathbf{1}$  and it follows that

$$(45) \quad \mathbf{x}^T \sigma_b(\Gamma) \mathbf{x} = (\mathbf{x} - (\mathbf{1}^T \mathbf{x}) \mathbf{b})^T \sigma(\Gamma) (\mathbf{x} - (\mathbf{1}^T \mathbf{x}) \mathbf{b}) \geq 0,$$

with strict inequality if  $\mathbf{x} - (\mathbf{1}^T \mathbf{x}) \mathbf{b} \neq \mathbf{0}$ . However,  $\mathbf{x} \perp \mathbf{b}$  and  $\mathbf{b}^T \mathbf{1} = 1$  implies that  $\mathbf{x}$  is not parallel to  $\mathbf{1}$  and so we must have strict positivity in (45).  $\square$

**A.3. Variograms in the positive case.** In our study of total positivity for extremes we showed in Lemma 4.5 that a particularly important case is when  $\Theta_{ij} \leq 0$  for all  $i \neq j$ . This is the case when  $\Theta$  corresponds to a Laplacian matrix on a connected graph with positive weights on each edge. In this case  $Q_{ij} = -\Theta_{ij} \geq 0$  for all  $i \neq j$ .

Recall from Remark A.6 and Lemma A.7 that if  $\Gamma \in \mathcal{C}^d$  then  $\Gamma$  is always a distance matrix in the sense that  $\sqrt{\Gamma_{ij}}$  are distances between a finite collection distinct points  $\mathbf{y}_i$  for  $i = 1, \dots, d$ , that lie in some Euclidean space  $\mathbb{R}^p$ . Let  $U \in \mathbb{R}^{p \times d}$  be a matrix whose columns are  $\mathbf{y}_1, \dots, \mathbf{y}_d$ . Note that translating all points  $\mathbf{y}_i$  will not change mutual distances. We consider two important cases:

Case 1: We translate the points by their average so that now  $\sum_i \mathbf{y}_i = \mathbf{0}$ . In this case the Gram matrix  $U^T U$  lies in  $\mathbb{U}$  and in fact it is equal to  $\Sigma = \sigma(\Gamma)$ .

Case 2: We translate the points to move one of the points to the origin so that now  $\mathbf{y}_k = \mathbf{0}$  for some  $k = 1, \dots, d$ . In this case  $U^T U \in \mathbb{U}_k$  and in fact it is equal to  $\tilde{\Sigma}^{(k)} = \sigma_k(\Gamma)$ .

In what follows we outline some of interesting results of Miroslav Fiedler; see [Fiedler \(1998\)](#) and also an excellent overview in [Devriendt \(2020\)](#). Note that if  $\Gamma \in \mathcal{C}^d$  then  $\Sigma$  and  $\tilde{\Sigma}^{(k)}$  have rank  $d - 1$ . It implies that we can assume  $k = d - 1$ .

**Lemma A.9.** *If  $\Theta = \Sigma^+$  is a Laplacian matrix of a weighted graph (with nonnegative weights) then  $\Sigma = U^T U$ , where  $U \in \mathbb{R}^{(d-1) \times d}$  and the columns of  $U$  are vertices of a simplex, whose polar is hyperacute.*

For the proof see Lemma 1 in [Devriendt \(2020\)](#).

As pointed in Section D of [Devriendt \(2020\)](#), if  $\Theta$  is a Laplacian matrix of a graph then the entries of the corresponding matrix  $\Gamma$  are the effective resistances, and  $\Gamma$  is called the resistance matrix. The effective resistance allows the bijection between simplices, graphs and Laplacian matrices to be summarized beautifully by the following identity (see Theorem 2 in [Devriendt \(2020\)](#)).

**Theorem A.10** (Fiedler's identity). *For a weighted graph with Laplacian  $\Theta$  and resistance matrix  $\Gamma$  the following identity holds*

$$(46) \quad -\frac{1}{2} \begin{bmatrix} 0 & \mathbf{1}^T \\ \mathbf{1} & \Gamma \end{bmatrix} = \begin{bmatrix} 4R^2 & -2\mathbf{r}^T \\ -2\mathbf{r} & \Theta \end{bmatrix}^{-1},$$

where  $\mathbf{r} = \frac{1}{2}\Theta\xi + \frac{1}{d}\mathbf{1}$  with  $\xi = \text{diag}(\Sigma)$ , and  $R = \sqrt{\frac{1}{2}\xi^T(\mathbf{r} + \frac{1}{d}\mathbf{1})}$ .

As we noted above,  $\sqrt{\Gamma_{ij}}$  are always distances in the sense that the map  $(i, j) \mapsto \sqrt{\Gamma_{ij}}$  is a metric function. However, if  $\Theta$  is a Laplacian matrix then the entries of  $\Gamma$  are effective resistances. By the next lemma we can conclude that, in this special case, the entries of  $\Gamma$  form a metric (see [Klein and Randić \(1993\)](#)).

**Lemma A.11.** *If  $\Theta_{ij} \leq 0$  for all  $i \neq j$  then the effective resistance  $(i, j) \mapsto \Gamma_{ij}$  is a metric function.*

The implication in Lemma 4.6 cannot be reversed. There are situations when  $\Gamma$  is a metric but  $\Theta$  is not a Laplacian of a graph. In Proposition 4.6 we discussed exact conditions when it happens together with a probabilistic interpretation in terms of the extreme association.

The fact that  $(i, j) \mapsto \Gamma_{ij}$  is a metric does not give us a way to realize this metric as an Euclidean distance metric. The case we find particularly interesting is related with tree metrics (see, e.g., [Semple et al. \(2003\)](#)). Let  $T$  be an undirected tree with  $d$  leaves labeled with  $[d]$ . We say that  $\Gamma \in \mathbb{S}_0^d$  forms a tree metric over  $T$  if there exists edge length assignment  $\theta_{uv} \geq 0$  for  $uv \in T$  such that

$$(47) \quad \Gamma_{ij} = \sum_{uv \in \text{ph}(i, j; T)} \theta_{uv},$$

where  $\text{ph}(i, j; T)$  denotes the unique path between  $i$  and  $j$  in  $T$ .

Let  $T^k$  denote a rooted tree obtained from  $T$  by directing all edges away from a leaf  $k \in [d]$ . Note that

$$(48) \quad \tilde{\Sigma}_{ij}^{(k)} = \frac{1}{2}(\Gamma_{ik} + \Gamma_{jk} - \Gamma_{ij}) = \sum_{uv \in \text{ph}(i \wedge j, T^k)} \theta_{uv},$$

where  $i \wedge j$  denotes the most recent common ancestor of  $i$  and  $j$  in the tree  $T^k$ . But this means that the entries of  $\Sigma^{(k)}$  lie in the Brownian motion tree model on the tree  $T^k$ ; see [Sturmfels et al. \(2020\)](#) for more details. We get the following result.

**Proposition A.12.** *The image under  $\sigma_k$  of the set of all tree metrics over a given tree  $T$  is equal to the set of covariance matrices of the Brownian motion tree model over the rooted tree  $T^k$ .*

We finish by noting that the observation that the square root of a tree metric has an Euclidean embedding (which is a side product of this analysis) has been important for understanding some algorithms in phylogenetics [Layer and Rhodes \(2017\)](#).

## APPENDIX B. AUXILIARY RESULTS AND PROOFS

### B.1. Auxiliary results.

**Lemma B.1.** *The function  $f$  is strongly  $MTP_2$  if and only if for all  $\mathbf{x}, \mathbf{y} \in \mathbb{R}^d$ , and for all  $s, t \geq c$  (for some  $c \in \mathbb{R}$ )*

$$(49) \quad f(\mathbf{x} - s\mathbf{1})f(\mathbf{y} - t\mathbf{1}) \leq f(\mathbf{x} \vee \mathbf{y} - (s \vee t)\mathbf{1})f(\mathbf{x} \wedge \mathbf{y} - (s \wedge t)\mathbf{1}).$$

*Proof.* We first show that the strongly  $MTP_2$  condition (2) implies the alternative (49). Suppose  $t \geq s \geq c$ . Let  $\tilde{\mathbf{x}} = \mathbf{y} - t\mathbf{1}$ ,  $\tilde{\mathbf{y}} = \mathbf{x} - s\mathbf{1}$ , and  $\alpha = t - s \geq 0$ . We have  $\tilde{\mathbf{x}} + \alpha\mathbf{1} = \mathbf{y} - s\mathbf{1}$  and  $\tilde{\mathbf{y}} - \alpha\mathbf{1} = \mathbf{x} - t\mathbf{1}$ . By (2)

$$f(\mathbf{x} - s\mathbf{1})f(\mathbf{y} - t\mathbf{1}) = f(\tilde{\mathbf{x}})f(\tilde{\mathbf{y}}) \leq f((\tilde{\mathbf{x}} + \alpha\mathbf{1}) \wedge \tilde{\mathbf{y}})f(\tilde{\mathbf{x}} \vee (\tilde{\mathbf{y}} - \alpha\mathbf{1})) = f(\mathbf{x} \wedge \mathbf{y} - s\mathbf{1})f(\mathbf{x} \vee \mathbf{y} - t\mathbf{1}),$$

which is exactly (49). If  $c \leq t < s$  then we proceed in exactly the same way taking  $\tilde{\mathbf{x}} = \mathbf{x} - s\mathbf{1}$ ,  $\tilde{\mathbf{y}} = \mathbf{y} - t\mathbf{1}$ , and  $\alpha = s - t \geq 0$ . This proves one implication. The other implication is obtained by reversing this argument. Fix  $\mathbf{x}, \mathbf{y}$ , and  $\alpha \geq 0$ . Suppose that (49) holds and take  $\tilde{\mathbf{x}} = \mathbf{x} + s\mathbf{1}$ ,  $\tilde{\mathbf{y}} = \mathbf{y} + t\mathbf{1}$ ,  $t = c$ ,  $s = c + \alpha$ . Then, by (49),

$$f(\mathbf{x})f(\mathbf{y}) = f(\tilde{\mathbf{x}} - s\mathbf{1})f(\tilde{\mathbf{y}} - t\mathbf{1}) \leq f(\tilde{\mathbf{x}} \wedge \tilde{\mathbf{y}} - t\mathbf{1})f(\tilde{\mathbf{x}} \vee \tilde{\mathbf{y}} - s\mathbf{1}) = f((\mathbf{x} + \alpha\mathbf{1}) \wedge \mathbf{y})f(\mathbf{x} \vee (\mathbf{y} - \alpha\mathbf{1})),$$

which is exactly (2).  $\square$

**Proposition B.2.** *We have:*

- (i) *If  $\mathbf{X}$  is associated then any subvector of  $\mathbf{X}$  is associated.*
- (ii) *If  $\mathbf{X}' \perp\!\!\!\perp \mathbf{X}''$  are associated then  $\mathbf{X} = (\mathbf{X}', \mathbf{X}'')$  is associated.*
- (iii) *Univariate random variables are associated.*
- (iv) *Non-decreasing functions of associated random variables are associated.*
- (v) *A Gaussian vector is associated if and only if its covariance matrix has only non-negative entries.*

*Proof.* Properties (i)-(iv) are the properties (P1)-(P4) in [Esary et al. \(1967\)](#). Property (v) is the main result in [Pitt \(1982\)](#).  $\square$

**B.2. Proof of Theorem 5.3.**  $\mathbf{Y} \sim \mathbb{P}_{\mathbf{Y}}$  satisfies the pairwise Markov property with respect to  $G_e(\mathbb{P}_{\mathbf{Y}})$ . [Engelke and Hitz \(2020, Theorem 1\)](#) shows the equivalence of the pairwise and the global Markov property for extremal independence, therefore  $\mathbf{Y}$  satisfies the global Markov property with respect to  $G_e(\mathbb{P}_{\mathbf{Y}})$ . Assume disjoint  $A, B, C \subset V$ , such that  $C$  does not separate  $A$  from  $B$  in  $G(\mathbb{P}_{\mathbf{Y}})$ . If  $\mathbb{P}_{\mathbf{Y}}$  is extremal faithful to  $G(\mathbb{P}_{\mathbf{Y}})$ , it follows that  $\mathbf{Y}_A \not\perp\!\!\!\perp \mathbf{Y}_B \mid \mathbf{Y}_C$ . To see this, let  $kl \in E(\mathbb{P}_{\mathbf{Y}})$ , which means that  $Y_k \not\perp\!\!\!\perp Y_l \mid \mathbf{Y}_{V \setminus kl}$ . Now, upward-stability (see Theorem 5.1) implies that  $Y_k \not\perp\!\!\!\perp Y_l \mid \mathbf{Y}_C$ . As  $C$  does not separate  $A$  from  $B$ , there is a path in  $G_e(\mathbb{P}_{\mathbf{Y}})$  from some  $i \in A$  to some  $j \in B$  that does not intersect  $C$ . It holds that  $Y_k \not\perp\!\!\!\perp Y_l \mid \mathbf{Y}_C$  for any edge  $kl$  on the path from  $i$  to  $j$ . From singleton-transitivity (see Theorem 5.1) it follows that  $Y_i \not\perp\!\!\!\perp Y_j \mid \mathbf{Y}_C$ . This implies the theorem.

### B.3. Proof of Theorem 6.4.

**Lemma B.3.** *The dual problem (31) is feasible if and only if  $\bar{\Gamma}_{ij} > 0$  for all  $1 \leq i < j \leq d$ .*



*Proof.* We prove the right implication using the contrapositive statement. Suppose  $\bar{\Gamma}_{ij} = 0$  for some  $i \neq j$ . Then each feasible point  $\Gamma$  of (31) must satisfy  $\Gamma_{ij} = 0$  but then it cannot be strictly conditionally negative definite (see Lemma A.7 in Appendix A). For the left implication, let  $\epsilon = \min_{i \neq j} \bar{\Gamma}_{ij} > 0$ . Then  $\Gamma = \epsilon \mathbf{1}\mathbf{1}^T - \epsilon I$  is a feasible point. Indeed, clearly  $\Gamma \leq \bar{\Gamma}$  and conditional strict negative definiteness follows because for any nonzero  $\mathbf{x}$  such that  $\mathbf{x}^T \mathbf{1} = 0$  we have

$$\mathbf{x}^T \Gamma \mathbf{x} = -\epsilon \|\mathbf{x}\|^2 < 0.$$

□

Since the primal problem is always strictly feasible, Slater's condition imply strong duality that states that the optimal values of the primal and the dual problems are equal; see Section 5.2.3 in [Boyd and Vandenberghe \(2004\)](#).

We are now ready to prove Theorem 6.4.

*Proof of Theorem 6.4.* We prove the right implication using the contrapositive statement. Suppose  $\bar{\Gamma}_{ij} = 0$  for some  $i \neq j$ . By Lemma B.3 the dual problem is infeasible and so, by strong duality, it follows that the primal problem is unbounded and so the optimum does not exist. For the left implication, since the dual problem has a feasible point in the relative interior, the function  $f(Q)$  is bounded below for all  $Q \in \mathbb{U}_+$ . By the Weierstrass Theorem (e.g. Proposition 3.2.1 in [Bertsekas \(2009\)](#)) to show existence of the optimum, it is then enough to show that  $f$  is coercive and that it is a closed function, meaning that  $\{x : f(x) \leq \alpha\}$ . To show that it is coercive, it is enough to show that  $-\log \det \Theta^{(k)} + \text{tr}(S^{(k)} \Theta^{(k)}) \rightarrow \infty$  if  $\|\Theta^{(k)}\| \rightarrow \infty$ . Note that  $S_{ii}^{(k)} = \bar{\Gamma}_{ik} > 0$  and so the proof of this fact can be found in Appendix A of [Ravikumar et al. \(2011\)](#). To show that  $f$  is closed note that, since  $f$  is a proper convex function, closedness of  $f$  is implied by lower semi-continuity (see Section 7 in [Rockafellar \(2015\)](#)). To show lower semi-continuity note that  $f$  is continuous (and so lower-semicontinuous) for all  $Q \in \mathcal{K}^d$ . It remains to show that  $f$  is lower-semicontinuous at the boundary points of  $\mathcal{K}^d$  where the corresponding  $\Theta^{(k)}$  is positive semi-definite but not positive definite. Let  $Q_0$  be any such point. To prove lower semi-continuity, we need to show that for every sequence  $Q_i$  converging to  $Q_0$  the sequence  $f(Q_i)$  converges to  $+\infty$ . This is non-trivial only if the elements of the sequence  $(Q_i)$  all lie in  $\mathcal{K}^d$ . But in this case it is easy to see that the trace term converges to a finite number and the log-determinant term in  $-\ell(Q; \bar{\Gamma})$  converges to  $+\infty$ . □

Frank Röttger, Université de Genève, Switzerland, [frank.roettger@unige.ch](mailto:frank.roettger@unige.ch)

Sebastian Engelke, Université de Genève, Switzerland, [sebastian.engelke@unige.ch](mailto:sebastian.engelke@unige.ch)

Piotr Zwiernik, University of Toronto, ON, Canada, [piotr.zwiernik@utoronto.ca](mailto:piotr.zwiernik@utoronto.ca)